Bayesian approach to infer the duration of antibody seropositivity and neutralizing responses to SARS-CoV-2

Manuela Royer-Carenzi, Jean-Marc Freyermuth

Bayesian approach to infer the duration of antibody seropositivity and neutralizing responses to SARS-CoV-2

M. Royer-Carenzi[a] and J.-M. Freyermuth[a]

[a]Aix Marseille Univ, CNRS, Centrale Marseille, I2M, Marseille, France

ARTICLE HISTORY
Compiled January 20, 2023

Abstract

Estimating the duration of natural immunity induced by SARS-CoV2 infection is crucial in health policy strategies. A patient infected by the SARS-CoV2 quickly produces three antibody isotypes IgM, IgG, and IgA that reveal an infection. In this paper, we use a Bayesian two-component mixture of random coefficient model to capture the longitudinal/temporal evolution of antibody levels, as well as viral neutralization on the dataset reported by Seow et al. in [1]. We observe that the more severe the symptoms, the more intense antibodies and immunity responses. And their decline is decelerated with the severity. Moreover, it appears that viral neutralization is best predicted by the level of IgM or IgA antibody, rather than by IgG level. Furthermore, our model is particularly suitable to estimate the Probability of being Out of Detection. Thus, we observe that although antibodies persist for up to 5 months in the plasma, the probability of becoming undetectable exceeds 50% after 3 months.

KEYWORDS
COVID-19, antibody antigen, viral neutralization, Bayesian mixture model, posterior predictive distribution.

1. Introduction

The on-going Severe Acute Respiratory Syndrome Coronavirus 2 (SARS-CoV-2) pandemic stresses the need for quantitative methods for evaluating the duration of antibody persistence, particularly for assessing the likelihood of reinfection. General vaccination policies might benefit from such a method as infection waves succeed to each other.

A patient infected by the COVID-19 quickly produces three antibody isotypes, IgM, IgG, and IgA as expressions of prompt, long-lasting, and mucosal immunity, respectively [2, 3]. Numerous studies show a correlation between a high antibody production and the severity of symptoms [4–13]. Several techniques were developed for an easy antibody testing, such as kits for testing with finger-prick capillary blood (lateral flow assays LFAs). If a sufficiently high level of antibody is present, the test indicates that the result is positive; the patient is then declared seropositive, seronegative otherwise. But antibody response can be measured with more precision using enzyme-linked immunosorbent assay, such as ELISA protocol [6], and allows quantitative monitoring of antibody rates.

The presence of antibodies reveals an infection, even if the patient is symptomless. Therefore, using serological tests appears useful to estimate the prevalence of COVID-19 in a population. However, knowing the duration of antibody detectability is crucial to better estimate the prevalence of the disease. Indeed, antibodies gradually disappear until they become undetectable.

CONTACT J.-M. Freyermuth. Email: jean-marc.freyermuth@univ-amu.fr

In [11] Herrington studies the duration of antibody detectability to SARS-CoV-2 using longitudinal data, provided by rapid serological assays, where the response is either seropositive or seronegative. The percentage of observed-seropositive patients provides sequential estimates of covid-prevalence. Here, we use sequential serum samples collected by ELISA protocol reported by Seow et al. in [1]. We model the evolution of antibody rate, in order to estimate at each time the probability that this antibody becomes undetectable. Such a Probability of being Out of Detection is denoted as POD in the sequel. POD evolution will provide a modeling of the evolution of the covid prevalence in the medium term.
In this paper, we propose a Bayesian modeling of the longitudinal profile of antibody levels. This model can accommodate with possibly low samples sizes, it captures subject-specific deviations, and it allows computing the POD at a given future time. More specifically, we use a Bayesian two-component mixture of random coefficients models and get POD from the posterior predictive distribution. All results are obtained using the R-software `brms`.
Firstly, we establish a link between the latent process of belonging to one of the terms of the mixture, with the severity score. Secondly, we study the expected behavior of future observations, and specifically the expected maximum amplitude, ranked with respect to the severity score. From antibodies expected evolution, we quantify the antibody level that should be measured to ensure that the patient is still immune. Next, we compute POD at a long run time, to study the duration of antibody persistence.

2. Materials and Methods

2.1. Data description

In [1] Seow et al. provide a longitudinal study of antibody levels for 65 patients infected with COVID-19, confirmed with a SARS-CoV-2 by RT-PCR assays on nasal and pharyngeal swab specimen. An increasing severity score was assigned to every patient :

- Group 0 : Asymptomatic patient, or no requirement for supplemental oxygen;
- Group 1/2/3 : Requirement for supplemental oxygen, with fraction of inspired oxygen (FIO_2) ≤ 0.8 for at least 12 hours;
- Group 4 : Requirement for intubation and mechanical ventilation or supplemental oxygen, with fraction of inspired oxygen (FIO_2) > 0.8 and peripheral oxygen saturations $< 90\%$ for at least 12 hours;
- Group 5 : Requirement for ECMO.

Due to low sample sizes in the initial Groups 1, 2 and 3, we gathered these patients in a single group denoted as Group 1/2/3 hereafter. The authors measured the IgG, IgM and IgA response against S glycoprotein, RBD and N protein by enzyme-linked immunosorbent assay (ELISA) over multiple time points. Optical density (OD) was measured at 1:50 dilution, and a sample was considered as low when OD < 0.2 and high when OD > 0.4. The authors also measured SARS-CoV-2 neutralization potency, called peak infective dose or ID_{50}, using a pseudotyped HIV incorporating the S glycoprotein of SARS-CoV-2, with 50 as level detection. ID_{50} may be interpreted as a primary assessment of SARS-CoV-2 immunity response [14]. In the sequel, we perform our statistical modeling on the log-transformed data. Figure 2 displays longitudinal titers evolution for patients, and shows that whole IgG_S, IgM_S, IgA_S and Id50_PV titers have similar evolution, with a plateau feature.

2.2. Bayesian modeling principles

In this section, we provide an overview of the essential tools for Bayesian estimation of the (posterior) Probability Of non Detectability (POD). For pedagogical purposes, we first obtain

the POD for the standard linear regression with conjugate prior specification and then for the random coefficient model with vague prior. The latter case involves the use of Markov Chain Monte Carlo methods (MCMC) which principles are briefly described hereafter. Finally, we describe how to evaluate the POD for a two-component mixture of random coefficient models, which offers the best fit to our complex data. All analyses have been performed using the `brms` R-package [15].

2.2.1. Bayesian analysis in a nutshell

We adopt a fully Bayesian approach for our data analysis. Three main reasons motivated this choice. First, we have a restricted number of observations over the time for each subject, while comparatively many parameters will be needed to properly model the phenomenon and its variability. Second, we aim at performing prediction and getting uncertainty quantification. Third, the Bayesian framework is particularly well-adapted for mixture and for multilevel modeling.

In a (parametric) Bayesian framework, we specify a (parametric) probabilistic model on our data. We call it likelihood and write hereafter $p(y|\boldsymbol{\theta})$ where $\boldsymbol{\theta}$ is the vector of unknown parameters. The model parameters are treated as random variables, they are given prior probability distributions $\pi(\boldsymbol{\theta}) := \pi(\boldsymbol{\theta}\ |\boldsymbol{\theta}_0)$ defined on the parameter space denoted hereafter as Θ. $\boldsymbol{\theta}_0$ are called hyperparameters and are often assumed to be known. Bayesian inference consists in updating our knowledge about the (distribution of the) parameters using the Bayes theorem:

$$\pi(\boldsymbol{\theta}|y) = \frac{p(y|\boldsymbol{\theta})\pi(\boldsymbol{\theta})}{p(y)} \propto p(y|\boldsymbol{\theta})\pi(\boldsymbol{\theta}).$$

$\pi(\boldsymbol{\theta}|y)$ is the so-called posterior distribution of $\boldsymbol{\theta}$. $\propto$ stands for 'proportional up to a multiplicative constant' which does not depend on θ. The posterior distribution 'pools' all information about the parameters from the data and from the prior. In some specific situations this posterior distribution can be made explicit, but most of the time it requires Markov Chain Monte Carlo (MCMC) type algorithms to be exploited ([16]). Basically, those algorithms output (dependent) random draws from the posterior distribution, we denote them as $\left\{\boldsymbol{\theta}^{(m)},\ 1 \leq m \leq M\right\}$. Considering the Monte Carlo principle for dependent data, ergodic theorem applies, ensuring the convergence of empirical averages to the expectation $\mathbb{E}(g(\boldsymbol{\theta}))$ for any well-behaved function of the parameters $g(\cdot)$:

$$\frac{1}{M}\sum_{m=1}^{M} g(\boldsymbol{\theta}^{(m)}) \to \mathbb{E}(g(\boldsymbol{\theta})). \tag{1}$$

Typical examples are $g_1(x) = x,\ g_2(x) = x^2,\ g_3(x) = \mathbb{1}_{\{x\leq a\}}$, where notation $\mathbb{1}$ refers to the indicator function and a can be chosen such that $P\left(X \leq a\right) = 1-\alpha,\ \alpha \in]0,1[$. Posterior estimation of quantile allows us to evaluate two-sided Bayesian credible intervals at level $(1-\alpha)100\%$, i.e., an interval $[a,b]$ such that $\int_a^b \pi(\boldsymbol{\theta}|y)d\theta = 1-\alpha$ and $\int_{-\infty}^{a} \pi(\boldsymbol{\theta}|y)d\theta = \int_b^{+\infty} \pi(\boldsymbol{\theta}|y)d\theta = \alpha/2$. The Bayesian framework is particularly convenient for prediction and uncertainty quantification. A key quantity for model checking and prediction is the posterior predictive distribution. Consider a future observation $\tilde{y}$ arising from the same distribution as $y|\boldsymbol{\theta}$, assume that y and $\tilde{y}$ are conditionally independent given $\boldsymbol{\theta}$, denoted as $\tilde{y} \perp y|\boldsymbol{\theta}$, then the posterior distribution is given by:

$$p(\tilde{y}|y) = \int_{\boldsymbol{\Theta}} p(\tilde{y}|\boldsymbol{\theta})\pi(\boldsymbol{\theta}|y)d\boldsymbol{\theta}, \tag{2}$$

where Θ is the parameter space.

In practice, we can use the random draws from posterior distribution to get the distribution of $\tilde{y}|y$. More specifically, for each Monte Carlo iteration $1 \leq m \leq M$:

- generate $\boldsymbol{\theta}^{(m)}$ from the posterior distribution : $\boldsymbol{\theta}^{(m)} \sim \pi(\boldsymbol{\theta}|y)$,
- generate $\tilde{y}^{(m)}$ from the posterior distribution : $\tilde{y}^{(m)} \sim p\left(y|\boldsymbol{\theta}^{(m)}\right)$.

In the sequel, we assess model accuracy from graphical posterior predictive checks, as suggested in [17, 18]. It consists in checking the quality of the fit of the model by superposition of the data alongside the predictions from the fitted model. Furthermore, we consider two information criteria for model selection: the widely applicable information criterion (WAIC), introduced by Watanabe in [19] and the approximate leave-one-out cross-validation based on the posterior likelihood (looAIC) [19, 20].
In Section 2.2.4, our data models require the introduction of latent variables. The observations are then viewed as a marginal outcome from a more complex experiment involving unobserved, latent variables. They are modeled using a complete data likelihood that is denoted as $p^c(y, z|\boldsymbol{\theta})$, where $z \in \mathcal{Z}$ is a latent variable. Bayesian inference consists in obtaining the joint complete posterior and integrating out the latent variable to infer on the parameters.

$$\begin{aligned} \pi(\boldsymbol{\theta}|y) &= \int_{\mathcal{Z}} \pi(z, \boldsymbol{\theta}|y)dz = \int_{\mathcal{Z}} \frac{p^c(z, y|\boldsymbol{\theta})\pi(\theta)}{p(y)}dz \\ &\approx \int_{\mathcal{Z}} p(y|\boldsymbol{\theta}, z)p(z|\boldsymbol{\theta})\pi(\boldsymbol{\theta})dz. \end{aligned}$$

Under the assumption that the joint complete likelihood of the future observation is the same as the joint distribution of $y, z|\boldsymbol{\theta}$, we can derive the posterior predictive distribution in order to perform prediction, model assessment and ultimately to compute POD. As described in the next sections, the POD is obtained by exploiting the posterior predictive distribution in linear regression models. For the sake of clarity of our presentation, we describe it first in the simplest instance of standard linear regression with conjugate prior.

2.2.2. Simple regression model (LM)

The serum samples were collected on infected individuals, sequentially, at times $t_1, \cdots t_r$, providing a structural dependence between antibody level successively measured on a given patient. As shown in [1], and illustrated in Figure 2, antibody titers first increase, then reach a plateau before decreasing slightly. A quadratic function of time appears suitable for longitudinal antibody evolution. Thus, at a given time t_j, $j = 1, \cdots, r$ (number of days post onset symptoms), the antibody level is modeled with the following Bayesian linear model:

$$\begin{cases} y_{t_j}|\underline{b}, \sigma_\varepsilon^2 \overbrace{\sim}^{i.i.d} \mathcal{N}\left(\mu_{t_j}, \sigma_\epsilon^2\right), \\ \mu_{t_j} = b_0 + b_1\, t_j + b_2\, t_j^2, \end{cases} \tag{3}$$

where the parameter $\underline{b} = (b_0, b_1, b_2)'$ represents the global evolution of antibody titer (called fixed effect). The likelihood is given by $p(y|\boldsymbol{\theta}) = \prod_{j=1}^{T} p(y_{t_j}|\boldsymbol{\theta})$, where $\boldsymbol{\theta} = (\underline{b}, \sigma_\varepsilon^2)'$. If one considers the following prior specification, $(\underline{b}, \sigma_\varepsilon^2) \sim NIG(m, V, \gamma, \beta)$, then it is easy to show that the joint posterior distribution is $(\underline{b}, \sigma_\varepsilon^2)|y \sim NIG(m^*, V^*, \gamma^*, \beta^*)$, where the parameters $(m^*, V^*, \gamma^*, \beta^*)$ are a combination of prior, observations and design matrix information that we do not need to give explicit form here.
The posterior predictive distribution of a future observation at time t, $\widetilde{y}_t$, is directly obtained from Equation (2). In this precise example, it is a Generalized Student distribution $t_p(m^*, V^*, \gamma^*, \beta^*)$ (see [21]).
More generally, we are interested in two quantities:

- $E(t) := \mathbb{E}(\widetilde{y}_t \,|\, y)$, standing for the global behavior of a future observation;
- $POD(t, v) := \mathbb{P}\left(\widetilde{y}_t \leq v \,|\, y\right)$, representing the posterior POD, under threshold v, at time t, that can be denoted siwe mply $POD(t)$ when threshold v is known and fixed.

Both $E(t)$ and $POD(t, v)$ will be estimated as the average over Monte-Carlo iterations, possibly specified with a credible interval.

$$E(t) := \mathbb{E}(\widetilde{y}_t \,|\, y) = \int_{-\infty}^{+\infty} \widetilde{y}_t \, p(\widetilde{y}_t|y) d\widetilde{y}_t$$

$$= \int_{\boldsymbol{\Theta}} \int_{-\infty}^{+\infty} \widetilde{y}_t \, p(\widetilde{y}_t|\boldsymbol{\theta}) d\widetilde{y}_t \pi(\boldsymbol{\theta}|y) d\boldsymbol{\theta}; \tag{4}$$

$$POD(t, v) := \mathbb{P}\left(\widetilde{y}_t \leq v \,|\, y\right) = \int_{-\infty}^{v} p(\widetilde{y}_t|y) d\widetilde{y}_t$$

$$= \int_{\boldsymbol{\Theta}} \int_{-\infty}^{v} p(\widetilde{y}_t|\boldsymbol{\theta}) d\widetilde{y}_t \pi(\boldsymbol{\theta}|y) d\boldsymbol{\theta}. \tag{5}$$

The last integrals in Equations (4) and (5) are of the form of Equation (1) with

$$g_{E(t)}(\boldsymbol{\theta}) = \int_{-\infty}^{+\infty} \widetilde{y}_t \, p(\widetilde{y}_t|\boldsymbol{\theta}) d\widetilde{y}_t \quad \text{and}$$
$$g_{POD(t,v)}(\boldsymbol{\theta}) = \int_{-\infty}^{v} p(\widetilde{y}_t|\boldsymbol{\theta}) d\widetilde{y}_t.$$

Therefore $E(t)$ and $POD(t, v)$ can be approximated from posterior draws as follows

$$E(t) \approx \frac{1}{M} \sum_{m=1}^{M} \mathbb{E}\left(\widetilde{y}_t \,|\, \boldsymbol{\theta^{(m)}}\right); \tag{6}$$

$$POD(t, v) \approx \frac{1}{M} \sum_{m=1}^{M} \mathbb{P}\left(\widetilde{y}_t \leq v \,|\, \boldsymbol{\theta^{(m)}}\right), \tag{7}$$

where $\boldsymbol{\theta}^{(m)} = (\underline{b}^{(m)}, \sigma_\varepsilon^{2,(m)})'$ is generated from the joint posterior distribution $\pi(\boldsymbol{\theta}|y)$. Further-

more, Equations (3), (6) and (7) provide

$$E(t) \approx \frac{1}{M}\sum_{m=1}^{M}\mu_t^{(m)}; \tag{8}$$

$$POD(t,v) \approx \frac{1}{M}\sum_{m=1}^{M}\Phi\left(\frac{v-\mu_t^{(m)}}{\sigma_\varepsilon^{(m)}}\right), \tag{9}$$

where Φ is the standard Normal cumulative distribution function, and parameters $(\mu_t^{(m)}, \sigma_\varepsilon^{2,(m)})$ are expressed in Equation (3).

2.2.3. Random coefficient model (BLM)

Our previous modeling approach does not consider the potentially important patient-specific deviations in titers trajectories. We adopt the random coefficient model by introducing for each patient $1 \leq i \leq n$ the random coefficients $\underline{\beta}_i = \{(\beta_{0,i}, \beta_{1,i}, \beta_{2,i})\}$. Hence, the titer at time $t_{i,j}$ $(j = 1, \cdots, r_i)$ for subject i $(i = 1, \cdots, n)$ is modeled as follows:

$$\begin{cases} y_{i,t_{i,j}}|\underline{b}, \underline{\beta}_i, \sigma_\epsilon^2 \overbrace{\sim}^{i.i.d} \mathcal{N}\left(\mu_{t_{i,j}} + \nu_{i,t_{i,j}}, \sigma_\epsilon^2\right), \\ \mu_{t_{i,j}} = b_0 + b_1\, t_{i,j} + b_2\, t_{i,j}^2, \\ \nu_{i,t_{i,j}} = \beta_{i,0} + \beta_{i,1}\, t_{i,j} + \beta_{i,2}\, t_{i,j}^2, \end{cases} \tag{10}$$

with $\underline{\beta}_i|\Sigma_\beta \sim \mathcal{N}_3(0, \Sigma_\beta)$. We assume that random effects are independent, so that Σ_β is a diagonal matrix with diagonal denoted by (τ_0, τ_1, τ_2).

The likelihood $p(y|\boldsymbol{\theta}) = \prod_{i=1}^{n}\prod_{j=1}^{r_i} p(y_{i,t_{i,j}}|\boldsymbol{\theta})$, where $\boldsymbol{\theta} = \left(\underline{b}, \left\{\underline{\beta}_i\right\}_{i=1}^{n}, \sigma_\varepsilon^2\right)'$. We set the prior distributions on the unknown parameters to be as follows:

$$\begin{aligned} {}^t(b_0, b_1, b_2) &\sim \mathcal{N}_3(m, V), \\ \sigma_\varepsilon^{-2} &\sim \text{Half-Cauchy}(0, 50), \\ \Sigma_\beta^{-1} &\sim \mathcal{W}\text{ishart}_3(W, \nu), \end{aligned}$$

where $\nu > 0$ and V, W are definite-positive (3×3)-matrix.

We are still interested in both the expectation of a future observation for the subject i and its POD, denoted respectively by $E_i(t)$ and $POD_i(t,v)$, and defined as in Equations (4) and (5), but where $\widetilde{y}_t$ is replaced by $\widetilde{y_{i,t}}$. In the present case, the posterior is no longer analytically tractable, then we obtain these subject-specific quantities from the posterior draws, implementing this Bayesian model in the `brms` R-package. Following the same principle as in Equations (6) and (7), where $\widetilde{y}_t$ is replaced again by $\widetilde{y_{i,t}}$, and where $\boldsymbol{\theta}^{(m)} = (\underline{b}^{(m)}, \underline{\beta}_i^{(m)}, \sigma_\varepsilon^{2\,(m)})'$, we obtain an

expression for $E_i(t)$ and $POD_i(t,v)$ that are similar to Equations (8) and (9). Consequently,

$$\begin{aligned} E_i(t) &\approx \frac{1}{M}\sum_{m=1}^{M}\left(\mu_t^{(m)} + \nu_{i,t}^{(m)}\right); \\ POD_i(t,v) &\approx \frac{1}{M}\sum_{m=1}^{M}\Phi\left(\frac{v - \left(\mu_t^{(m)} + \nu_{i,t}^{(m)}\right)}{\sigma_\varepsilon^{(m)}}\right), \end{aligned}$$

where parameters $(\mu_t^{(m)}, \nu_{i,t}^{(m)}, \sigma_\varepsilon^{2,(m)})$ are expressed in Equations (10).

2.2.4. Two-component mixture of random coefficient models (BMLM)

Mixture of linear regressions were introduced to deal with non-linearity ([22–24]), and have been proved useful in many applications, such as in [25–27]. Our observations now consist of pairs $\left\{(y_{i,t_{i,j}}, z_{i,t_{i,j}}); 1 \leq i \leq n;\ 1 \leq j \leq r_i\right\}$, where the $z_{i,t_{i,j}}$'s are binary latent variables. They specify from which random coefficient model, labelled $\{A, B\}$, the observations $t_{i,j},\ 1 \leq j \leq r_i$, from patient i arise:

$$z_{i,t_{i,j}} = \begin{cases} 1, \text{ if } y_{i,t_{i,j}}|\underline{b}^{(A)}, \underline{\beta}_i^{(A)}, \sigma_\varepsilon^{2,(A)} \sim \mathcal{N}\left(\mu_{t_{i,j}}^{(A)} + \nu_{i,t_{i,j}}^{(A)}, \sigma_\varepsilon^{2,(A)}\right) \\ 0, \text{ if } y_{i,t_{i,j}}|\underline{b}^{(B)}, \underline{\beta}_i^{(B)}, \sigma_\varepsilon^{2,(B)} \sim \mathcal{N}\left(\mu_{t_{i,j}}^{(B)} + \nu_{i,t_{i,j}}^{(B)}, \sigma_\varepsilon^{2,(B)}\right). \end{cases}$$

The conditional distribution of the observations and latent variables can be described as follows:

$$\begin{cases} y_{i,t_{i,j}}|\boldsymbol{\theta}, \lambda^{(A)} \sim \lambda^{(A)}\,\mathcal{N}\left(\mu_{t_{i,j}}^{(A)} + \nu_{i,t_{i,j}}^{(A)}, \sigma_\varepsilon^{2,(A)}\right) + (1-\lambda^{(A)})\,\mathcal{N}\left(\mu_{t_{i,j}}^{(B)} + \nu_{i,t_{i,j}}^{(B)}, \sigma_\varepsilon^{2,(B)}\right), \\ z_{i,t_{i,j}}|\lambda^{(A)} \sim Be(\lambda^{(A)}), \quad \text{with} \quad z_{i,t_{i,j}} = z_{i,t_{i,j'}},\ \forall\ 1 \leq j, j' \leq r_i. \end{cases}$$

where $\lambda^{(A)} \in]0,1[$ and coefficients $\mu_{t_{i,j}}^{(A)}, \mu_{t_{i,j}}^{(B)}, \nu_{t_{i,j}}^{(A)}$ and $\nu_{t_{i,j}}^{(B)}$ are defined with the same expression as in Equation (10). and $\boldsymbol{\theta} = (\boldsymbol{\theta}^{(A)}, \boldsymbol{\theta}^{(B)})'$, with, $\boldsymbol{\theta}^{(K)} = \left(\underline{b}^{(K)}, \left\{\underline{\beta}_i^{(K)}\right\}_{i=1}^{n}, \sigma_\varepsilon^{2(K)}\right)'$, for $K \in \{A, B\}$. For notations simplicity, let us define $\lambda = (\lambda^{(A)}, \lambda^{(B)})$, where $\lambda^{(B)} = 1 - \lambda^{(A)}$. In addition, we introduce $Z_{i,t_{i,j}}$ with values in $\{A, B\}$ such that $z_{i,t_{i,j}} = \mathbb{1}_{\{Z_{i,t_{i,j}}=A\}}$. The complete data likelihood is

$$p^c(y, z|\boldsymbol{\theta}, \lambda^{(A)}) = \prod_{i=1}^{n}\prod_{j=1}^{r_i}\prod_{K\in\{A,B\}}\left(\lambda^{(K)}\,p(y_{i,t_{i,j}}|\boldsymbol{\theta}^{(K)})\right)^{\mathbb{1}_{\{z_{i,t_{i,j}}=K\}}}.$$

For the sake of brevity, we do not write down the prior specification that is setted up similarly as in Section 2.2.3. Just remark that the standard prior to be put on the parameter $\lambda^{(A)}$ is a beta distribution. The posterior distribution in this case is not tractable and MCMC strategies are developed to obtain posterior draws from which we will obtain the predictive posterior distribution. From Equation (2),

$$
\begin{aligned}
p(\tilde{y}_{i,t}|y) &= \int_{\Theta} p(\tilde{y}|\theta)\pi(\theta|y)d\theta \\
&= \int_{\boldsymbol{\Theta}} \left(\sum_{K\in\{A,B\}} p(\tilde{Z}_{i,t}=K) p(\tilde{y}_{i,t}|\boldsymbol{\theta}^{(K)})\, \pi(\boldsymbol{\theta}^{(K)}|y) \right) d\boldsymbol{\theta},
\end{aligned}
$$

The posterior predictive distribution in the BMLM is obtained as follows. For each $1 \leq m \leq M$:

- $\tilde{z}_{i,t}^{(m)} \sim p(\tilde{z}_{i,t}|\lambda^{(A,m-1)}, y)$,
- $\boldsymbol{\theta}^{(m)} \sim \pi(\boldsymbol{\theta}|\tilde{z}_{i,t}^{(m)}, y)$,
- $\tilde{y}_{i,t}^{(m)} \sim p(\tilde{y}_{i,t}|\tilde{z}_{i,t}^{(m)}, \boldsymbol{\theta}^{(m)})$.

The posterior probability for an observation to be labelled A or B, is estimated by Monte-Carlo:

$$
\mathbb{P}(Z_{i,t_{i,j}} = A) \approx \frac{1}{M} \sum_{m=1}^{M} \lambda_{i,t_{i,j}}^{(A,m)},
$$

where, $\lambda_{i,t_{i,j}}^{(A,m)}$ denotes the posterior probability that the observation $y_{i,t_{i,j}}$ originates from component A, when using parameters $\boldsymbol{\theta}^{(A,m)}$, obtained in the m_{th}-posterior draw :

$$
\lambda_{i,t_{i,j}}^{(A,m)} = \frac{\lambda^{(A,m)}\, p(y_{i,t_{i,j}}|\boldsymbol{\theta}^{(A,m)})}{\sum_{K\in\{A,B\}} \lambda^{(K,m)}\, p(y_{i,t_{i,j}}|\boldsymbol{\theta}^{(K,m)})}. \tag{11}
$$

Note that to ensure parameters identifiability, we impose that $\forall m,\ b_1^{(A,m)} < b_1^{(B,m)}$. Then we obtain

$$
\lambda^{(A)} \approx \frac{1}{M\sum_{i=1}^{n} r_i} \sum_{m=1}^{M} \sum_{i=1}^{n} \sum_{j=1}^{r_i} \lambda_{i,t_{i,j}}^{(A,m)}.
$$

As previously, we approximate the expectation of a future observation for the subject i, and its POD by

$$
E_i(t) \approx \frac{1}{M} \sum_{m=1}^{M} \sum_{K\in\{A,B\}} \lambda^{(K,m)} \times \left(\mu_t^{(K,m)} + \nu_{i,t}^{(K,m)} \right); \tag{12}
$$

$$
POD_i(t,v) \approx \frac{1}{M} \sum_{m=1}^{M} \sum_{K\in\{A,B\}} \lambda^{(K,m)} \Phi \left(\frac{v - \left(\mu_t^{(K,m)} + \nu_{i,t}^{(K,m)} \right)}{\sigma_{\varepsilon}^{(K,m)}} \right). \tag{13}
$$

where parameters $(\mu_t^{(K,m)}, \nu_{i,t}^{(K,m)}, \sigma_{\varepsilon}^{2\,(K,m)})$, for $K \in \{A, B\}$, are expressed in Equations (10).

Finally, let us introduce

$$E_i^{(m)}(t) := \sum_{K\in\{A,B\}} \lambda^{(K,m)} \left(\mu_t^{(K,m)} + \nu_{i,t}^{(K,m)}\right); \tag{14}$$

$$POD_i^{(m)}(t,v) := \sum_{K\in\{A,B\}} \lambda^{(K,m)} \Phi\left(\frac{v-\left(\mu_t^{(K,m)}+\nu_{i,t}^{(K,m)}\right)}{\sigma_\varepsilon^{(K,m)}}\right). \tag{15}$$

3. Results

3.1. Mixture is suitable

Using `brms` R-package, introduced by B¨urkner in [15], we studied the logarithm of IgG, IgM, IgA and ID50 titers either with a (BLM) or with a (BMLM) model, as defined respectively in Subsections 2.2.3 and 2.2.4. We consider a quadratic time-regression both for fixed and for random effects, nesting random effects within patients. Moreover, we take population-level priors as Gaussians, whereas standard deviation parameters are taken following a half Student-t prior with 3 degrees of freedom and a large scale parameter, equal to 10, which ensures non-negativity and a non-informative prior.

We assess model accuracy from posterior predictive checks, as suggested by Gelman et al. in [17]. It consists in drawing simulated values from the posterior predictive distribution (see Equation (2)) and in comparing them to the real data. A good model should exhibit small discrepancies between real and simulated data. In the Figure 4, we superimpose the real data distribution and 10 draws from the posterior predictive distribution, denoted respectively as y and y_{rep}. The first column displays the posterior predictive checks for the random coefficient models **(BLM)**. It reveals that it cannot capture neither the heavy-tailed left-skewed distribution of antibody titers nor the bimodal distribution of ID50 titer. On the contrary, Bayesian Mixture of Linear Model **(BMLM)** provides better abilities to fit the data, as shown on the second column of the Figure 4. Moreover, this feature is corroborated by model selection criteria of the Table 1 which largely favor the **(BMLM)** over the **(BLM)**. Consequently, involving a mixture of regressions is more accurate for all the antibody and ID50 titers.

Note that even if we allow correlations between the parameters of the coefficients of the model **(BMLM)**, when running model estimation, coefficients are not significantly correlated. So we can assume that they are uncorrelated.

We have demonstrated the need for a two-component mixture model. Nevertheless, the nature of the latent process remains to elucidate. Some exogenous variables may induce differences in either antibody or immune response. We have extracted the membership probabilities $\lambda_{i,t_{i,j}}^{(A,m)}$ associated to every observation, as introduced in Equation (11). We confronted membership probabilities and the only exogenous variable at our disposal, i.e. the severity score of the patient to whom the observation is associated. For each replicate, we estimated the probability that a severity score SS_k was associated with group A by averaging the realizations of the latent values by severity score. In other words, we consider

$$\lambda_{SS_k}^{(A,m)} = \frac{1}{r_{SS_k}} \sum_{i\in SS_k} \sum_{j=1}^{r_i} \lambda_{i,t_{i,j}}^{(A,m)},$$

where $r_{SS_k} = \sum_{i\in SS_k} r_i$ designates the total number of observations associated with patients whose severity score is SS_k. Figure 3 displays these membership probabilities by severity score for each antibody. We can see that each severity group has homogeneous membership probabilities, and that they even manage to discriminate patients according to their severity score. Thus,

for IgM and IgA antibodies, and a little less distinctly for IgG, each severity group has well differentiated probabilities. This is also true for Id50, when comparing symptomatic patients. Thus, the latent variable is very strongly related to the severity score, but there remains another underlying process that explains the evolution Id50 levels for asymptomatic patients. We deduce that patient's classification is directly related with severity score for antibody level, whereas heterogeneity in immune response results from a more complex process.

3.2. Individual long-term evolution

3.2.1. Behavior comparison between severity scores

As the best model, **(BMLM)** is used to infer posterior predictive distribution for the logarithm of antibodies and Id50 titers. In this subsection, we study the expectation of a future observation, denoted by $E_i(t)$. By taking t from one day up to 180 after infection, and by computing the exponential, we infer the global long-term evolution for a future observation. Figure **??** displays the exponential estimations $\mathcal{E}_i(t) := e^{E_i(t)}$, averaged by disease severity group. Figure **??** shows that, in agreement with [1, 4], similar kinetics of antibody responses are observed, with an initial peak, followed by a declining phase, but with various amplitudes. Specifically, we compare the Maximum Amplitude (MA) for exponential evolutions $\mathcal{E}_i$, between severity score groups. Let us recall, from Equation (12), that $E_i(t)$ is defined as the average of the $M = 7\,000$ draws $E_i^{(m)}(t), m = 1, \cdots, M$. Furthermore, Equation (14) expresses $E_i^{(m)}(t)$ according to the estimated parameters value $\boldsymbol{\theta}^{(m)}$:

$$E_i^{(m)}(t) \;=\; a_{i,0}^{(A,m)} \;+\; a_{i,1}^{(A,m)}\, t \;+\; a_{i,2}^{(A,m)}\, t^2\,,$$

where, for $k = 0, 1, 2$,

$$a_{i,k}^{(m)} \;=\; \sum_{K\in\{A,B\}} \lambda^{(K,m)}\,(b_k^{(K,m)} + \beta_{i,k}^{(K,m)})\,.$$

Then the maximum amplitude is reached at time $-\dfrac{a_{i,1}^{(m)}}{2\,a_{i,2}^{(m)}}$, and is equal to

$$MA_i^{(m)} \;:= e^{\,a_{i,0}^{(m)} - \frac{\left(a_{i,1}^{(m)}\right)^2}{4\,a_{i,2}^{(m)}}}\,.$$

We then define the maximum amplitude associated to every patient i as

$$MA_i \;:=\; \frac{1}{M}\sum_{m=1}^{M} MA_i^{(m)}\,.$$

To compare maximum amplitudes between severity-score groups, we use posterior chains to estimate the probabilities that the MA of an SS_k-patient to be lower than the MA of an SS_l-patient, when $k < l$. For a given iteration m, and any time t, we denote by $\Pi_{k \text{ vs } l}^{\text{MA}\,(m)}(t)$ the proportion of times an SS_k patient has a lower MA than an SS_l patient, over all SS_k- versus SS_l-patient pairs. In other words,

$$\Pi_{k \text{ vs } l}^{\text{MA}\,(m)} \;=\; \frac{1}{n_k \times n_l} \sum_{i\in SS_k,\, h\in SS_l} \mathbb{1}_{MA_i^{(m)} < MA_h^{(m)}}\,.$$

The probability of an SS_k patient having a lower MA than an SS_l patient is then calculated by averaging over the M draws, and denoted by $\Pi^{\text{MA}}_{k \text{ vs } l}$. In the same way, a 80%-credibility interval, is computed from quantile samples. Table 2 displays MA comparison probabilities between severity scores. By displaying values higher than 0.5, Table 2 confirms, as observed in particular cases in [4–13], that the lower the severity score, the lower the MA. Thus, asymptomatic patients globally have a lower response (all $\Pi^{\text{MA}}_{0 \text{ vs } k} > 0.5$, for k=1/2/3, 4 and 5). But we observe in addition that this process remains true for all the other comparisons, except when comparing most severely affected patients (SS_4 against SS_5) for IgM and ID50 titers. In conclusion, we obtain that the more severely the patient is affected, the more important the amplitude for both IgG and IgA antibodies. It remains true for IgM and ID50 titers, except that severely affected patient (severity score "4" versus "5"), show an atypic behavior for these titers. Then, it should be noted that the more severely affected a patient is, the higher the peak protection, except for very severely affected patients who lose this immune advantage compared to severely affected patients. In terms of immunity, it seems advantageous to be highly affected, but not too much.

3.2.2. Immunity predicted from antibody titers

Rapid antigenic tests can reveal whether an individual has ever been in contact with the virus, by indicating the presence or absence of specific antibodies, such as IgG and/or IgM. But does antibody presence mean immunity ? More precisely, what is the minimum antibody level that should be measured to ensure that the patient is still immune ? In other words, what is the relevance of a diagnosis that concludes that a patient is immune as soon as his antibody level exceeds a certain threshold ? To investigate this question, we explore a large set of thresholds, and evaluate diagnosis on the individual long-term estimates previously generated. For each type of antibody IgX (with X=G, M or A), 500 thresholds (denoted as $v_{X,1}, \cdots v_{X,500}$) are set that scan the range of estimated values from 0 to 180 days for that antibody IgX, for all individuals combined. The question is whether this threshold $v_{X,j}$ for antibody IgX is appropriate to ensure immunity. In other words, does $IgX > v_{X,j}$ really imply $Id50 > 50$?

The relevance of a diagnostic test is evaluated by its sensitivity and specificity. In our case, test sensitivity is the probability that the test will be positive if the person is truly immune. It is the number of true positives (estimates with IgX antibody above the given threshold $v_{X,j}$ in immunized persons at the same time, i.e. with $Id50 > 50$) divided by the total number of estimates under immunity. Whereas, specificity is the probability that the test will be negative for a person who is not immune. It is the proportion of true negatives (estimates with IgX antibody below the given threshold $v_{X,j}$ in not-immunized persons at the same time, i.e. with Id50 below 50) among all non-immune estimates. Note that an optimal diagnosis has both a sensitivity and a specificity equal to 1, whereas a random guess means that sensitivity and specificity are equal to 0.5.

In Figure 5, we construct a ROC curve for antibodies IgG, IgM and IgA, by plotting sensitivity versus 1-specificity computed at thresholds $v_{X,j}$ with $j = 1, \cdots, 500$. The optimal diagnosis is located in the upper left corner. The closer the points on the ROC curve to the ideal coordinate, the more accurate the test is. As expected, Figure 5 shows that antibody diagnosis is not optimal, but its relevance highly depends on the threshold taken as seropositivity-limit. With the current limit fixed at 0.4, IgM turns out to be the least efficient, followed by IgG, and IgA being the most reliable (resp. distances from usual diagnosis to the theoretical optimal diagnosis $d_{\blacksquare,IgG} = 0.51, d_{\blacksquare,IgM} = 0.52$ and $d_{\blacksquare,IgA} = 0.42$). Unfortunately, IgA titer is rarely sought in the usual blood tests. But, choosing the convenient limit for seropositivity, given as $v_{IgM} = 0.921$ makes IgM titer as efficient as IgA (resp. distances from antibody-titers optimal diagnosis to the theoretical optimal diagnosis $d_{\bullet,IgG} = 0.49, d_{\bullet,IgM} = 0.40$ and $d_{\bullet,IgA} = 0.40$). We thus find the same results as in [28] which indicate that immunity is associated with IgM.

3.3. POD at a long run time

The duration of antibody persistence is an important issue [7], especially in assessing the likelihood of reinfection. Some authors [7, 11, 29, 30] attempt to answer this question by observing patients sequentially and either averaging or calculating the proportion of seropositive patients at each sampling time. In this paper, we propose a more subtle approach based on a proper modeling of the levels of antigen.
We use the $M = 7\,000$ posterior draws to compute the probability of a given patient to be seronegative at any time t, that we called Probability to be Out of Detection, and denoted by POD. Given the m^{th} realization of a posterior chain, we use Equation (15) to calculate, for each patient i, for each time t, the probability $POD_i^{(m)}(t)$, that the considered titer has a value lower than its associated detection-threshold. Next, as in Equation (13), we compute $POD_i(t)$ the mean of these probabilities, averaged on the M draws, for a given patient i, at a given time t.

To illustrate the effect of severity score on POD evolution, we average the POD values by severity score. In other words, at any time t, for any draw m, we denote by $POD_{SS_k}^{(m)}(t)$ the mean of the POD of the n_k patients with severity score SS_k :

$$POD_{SS_k}^{(m)}(t) \;=\; \frac{1}{n_k} \sum_{i \in SS_k} POD_i^{(m)}(t)\,. \tag{16}$$

Next, we can average $POD_{SS_k}^{(m)}(t)$ on the M draws, which is equal to the mean of individual PODs, within a given severity score. In other words,

$$POD_{SS_k}(t) \;=\; \frac{1}{M} \sum_{m=1}^{M} POD_{SS_k}^{(m)}(t) \tag{17}$$

$$\;=\; \frac{1}{n_k} \sum_{i \in SS_k} POD_i(t)\,. \tag{18}$$

As described in Equation (18), POD_{SS_k} evolution represents the average behavior of the POD within each severity-score group. Figure 6 displays $POD_{SS_k}(t)$ over a period of up to six months. It shows that the lower the severity score, the higher the POD. This is due to the fact that a low safety score is associated with a low level of antibodies, thus more easily undetectable. Moreover, for IgG, IgM and IgA antibodies, asymptomatic individuals are distinguished from the others by a curve far above those associated with the other severity scores. Note that this effect is more marked and more durable for IgA. On the other hand, for ID50 titer, we observe that it is the weakly affected patients (with a severity level equal to "0" or "1/2/3") who stand out, at least during 3 monthes.

Table 3 provides POD values averaged by severity score at specific times. The main values are $POD_{SS_k}(t)$, as defined in Equation (17), and specified with a 80%-credibility interval. In details, the 10%-quantile, such as the 90%-quantile are calculated from the M posterior draws of $POD_{SS_k}^{(m)}(t)$, defined in Equation (16). Table 3 confirms that a lower severity score is globally associated with a higher POD. In table 3, credibility intervals overlap for IgG and IgM titers. It is therefore not possible to assess whether the difference is significant. But it appears clearly that for IgA, POD is significantly higher for asymptomatic patients with respect to the others, up to at least two months, whereas for ID50, slightly affected patients (with severity score "0" or "1/2/3") have a higher POD during only one month. Globally, the difference between the groups tends to decrease over time.

Moreover, we also provide global behaviors, by averaging overall the patients, whatever its

severity score. Let us denote by n the total patients number, and introduce, for any draw m,

$$POD^{(m)}(t) \;=\; \frac{1}{n}\sum_{i=1}^{n} POD_i^{(m)}(t)\,.$$

We further denote by $POD(t)$ the value averaged over the M draws. Note that $POD(t)$ is also equal to the average of $POD_{SS_k}(t)$ values weighted by n_k, the number of patients in each severity-score group. We additionally compute 10%- and 90%-quantiles from $POD^{(m)}(t)$. In Table 3, lines referred to as "GLOBAL" in Table 3 display $POD(t)$ values, specified with their associated 80%-credibility score. We observe that after 6 months, the antibodies become undetectable for most patients (around 74% for IgG, 82% for IgM and 80% for IgA), but that immunity is still present for nearly half of them (47%). Consequently, the IgM-response is less durable than the IgG-response, as observed by Herrington in [11].

To determine whether POD difference between severity-score groups is significant, in an accurate way, we use posterior chains to estimate the probabilities that the POD of an SS_k-patient to be higher than the POD of an SS_l-patient, when $k < l$. For a given draw m, and any time t, we denote by $\Pi_{k \text{ vs } l}^{\text{POD}\,(m)}(t)$ the proportion of times an SS_k patient has a higher POD than an SS_l patient, over all SS_k- versus SS_l-patient pairs. In other words,

$$\Pi_{k \text{ vs } l}^{\text{POD}\,(m)}(t) \;=\; \sum_{i\in SS_k,\, h\in SS_l} \frac{\mathbb{1}_{POD_i^{(m)}(t) > POD_h^{(m)}(t)}}{n_k \times n_l}\,.$$

The probability of an SS_k patient having a higher POD than an SS_l patient is then calculated by averaging over the M draws, and denoted by $\Pi_{k \text{ vs } l}^{\text{POD}}(t)$. In the same way, a 80%-credibility interval, is computed from quantile samples.

Supplementary Table S1 displays POD comparison probabilities between severity scores at specific moments, accounting for their long-term evolution. By displaying values higher than 0.5, it confirms that the lower the severity score, the higher the POD, in almost all cases. Here, Figure 7 displays the mean values $\Pi_{k \text{ vs } l}^{\text{POD}}(t)$, standing for the estimation of POD comparisons. It is striking to see that IgG- and IgA-detectability globally remains higher for patients with severity score SS_l than for less severely affected patients (with severity score SS_k, where $k < l$) at least 6 months, whatever the comparison pairs SS_k versus SS_l. This effect is also observable for immunity detection, in terms of ID50-detection, for at least 5 months, except when comparing together most poorly (resp. most severely) affected patients, that is SS_0 versus $SS_{1/2/3}$ (resp. SS_4 versus SS_5). Finally, IgM-detectability globally remains lower for asymptomatic patients than for others, during at least 6 months. As a conclusion, a previous infection by Covid-19 disease leaves traces in terms of antibodies, all the more easily detectable if the individual has been more severely affected, and this effect lasts at least 6 months. With regard to immunity, a previous infection by Covid-19 disease also generates a more pronounced immune response for more severely affected patients, during about 5 months; after this period, immune response becomes similar regardless of the severity with which the patient was affected.

4. Discussion

In this analysis, we retain a rather sophisticated two-component mixture of random coefficient models. The information criteria we considered as well as the graphical assessments of posterior predictive checks move in this direction. Being in a Bayesian framework, then offers us several advantages. In particular, we could estimate the POD by direct exploitation of the posterior draws. Moreover, as a full probabilistic model, it could cope with possibly small sample sizes.

We recall that the expectation of the posterior distribution stands for the estimated global behavior of each titer. By averaging estimates by severity score, we obtain a similar pattern in all titers evolution : a peak followed by a decay well below the detection limit. But we observe that the intensity and the persistence of antibodies expression, such as immunity response, are related to the severity of the symptoms. Asymptomatic patients show moderate and transient antibody expression while patients with a higher severity score show more intense and persistent antibody levels. Actually, disease severity correlates with risk factors such as age or gender [7, 31–33]. Consequently, antibody levels also correlate with such social factors.

In our study, more than half of the patients have an undetectable level as early as 2 or 3 months after infection. The relatively rapid decline in the presence of antibodies to a level too low to be detectable, and the high proportion of asymptomatic patients who do not get tested, suggests that the prevalence of SARS-CoV-2 is underestimated, as is its virulence [11]. Moreover note that in Herrington's study [11], the author exploits data from serological tests to quantify the persistence of IgG- and IgM-antibody presence after Covid-19 infection. Each individual performs multiple sequential serological tests (with in-home testing of finger-prick capillary blood), until six months after the first positive test. The author provides a Table with the percentage of seronegative patients at specific times, which seems similar to the line "GLOBAL" in our Table 3. But the results obtained are not directly comparable. Indeed, on the one hand, the author uses direct observations rather than a model. On the other hand, his data are binary (sero-positive versus sero-negative), thus less precise than our quantitative data. And finally, be careful not to transpose the results directly because the reference time is the date of the first positive test in Herrington's paper, whereas we consider the time since symptoms onset, which has a negligible impact for IgG-antibodies, but it may induce a shift in the time scale for IgM-antibodies, for which our initial time probably corresponds to the observations collected at one month in [11]. Nevertheless, Herrington obtains a percentage of seronegative patients beyond 6 months which is compatible with our results in the table (IgG: 71% in our range [0.58 ; 0.87], IgM: 93% corresponds to the high limit of our credibility interval [0.71 ; 0.92]). The advantage of our approach is to use a model to estimate the persistence of the antibody response, rather than direct observation. It is therefore not necessary to take samples from subjects for six months. About three months of observation is sufficient to predict long-term behavior. Our Bayesian mixture linear regression model could not apply to such binary data, but We could adapt our methodology, by using a Bayesian mixture for logistic regression.

In addition, there is also the question of the persistence of the immunity of a patient already affected by this disease. How fast does it decrease and is it related to the measured antibody level ? Thus we studied the relationship between antibody levels and patient immunity. It turns out that IgA and IgM antibodies are naturally more predictive of the patient's immunity than the IgG antibody, which is the most analyzed. On the other hand, to infer immunity from one of these antibody levels, a suitable threshold must be considered, which may be quite far from the usual thresholds, which are for example used in rapid serological tests.

5. Conclusion

Our study allows describing the evolution of the detectability of COVID-19, in particular according to the severity with which the patient was affected. We observe that a more severely affected patient keeps more marked traces in terms of presence of antibodies. Similarly, the immunity in terms of ID50 is globally less present in a patient with a low level of disease.

The POD study confirms the relatively rapid decrease of antibodies, which leads to a re-estimation of the prevalence of covid upwards, but its virulence downwards. However, it is important to note that the immunity unfortunately has the same decreasing trend while it stabilizes for a significant proportion of patients. This implies that immunity relies not only on

the presence of antibodies, but also on other processes such as T-cells, which could maintain immunity in the longer term.

Our methodology can be adapted to other types of data. For example, using data from Phase 3 clinical trials of a vaccine, it could be possible to determine the duration of the immune response produced by the candidate vaccine, possibly as a function of patient characteristics such as age or comorbidities. Binary data such as Herrington's are easier to obtain with in-home testing of finger-prick capillary blood, but less accurate than measuring the antibody value. Nevertheless, we have shown that they are not without interest. On the one hand, they can be used directly by adapting our methodology with a logistic regression. On the other hand, seropositivity to a specific antibody would allow inducing the persistence of an immunity, provided that adequate thresholds for seropositivity are chosen, these thresholds having been calibrated by a preliminary study.

Acknowledgement

The authors great fully acknowledge Vicky Merhej for her helpful discussions.

Disclosure statement

The authors report there are no competing interests to declare.

Biographical note

The authors contributed equally. Both authors are Associate Profesors in I2M laboratory, Aix Marseille University, France.

Manuela ROYER-CARENZI (ORCID: https://orcid.org/0000-0003-2392-1120) is Associate Profesor since 2004, and a fellow of I2M laboratory in Aix-Marseille University since 2007. She started working on Backward Stochastic Differential Equations, with a PhD in Rennes University, France (2003). Thanks to collaborations with biologists and actuaries, she gets interested in applied statistics, with main applications in Ecology, in Epidemiology and in Phylogeny.

Jean-Marc FREYERMUTH (ORCID: https://orcid.org/0000-0003-3539-716X) received his Ph.D degree in statistics from the Université Catholique de Louvain, Belgium, in 2011. He is currently an associate professor at Aix-Marseille University. His main research interests include wavelet methods, time series analysis and biostatistics.

Data availability statement

All data come from Seow et al. study [1], and are available from the following website https://www.nature.com/articles/s41564-020-00813-8
in Section Supplementary information.

References

[1] J. Seow, C. Graham, B. Merrick, S. Acors, S. Pickering, K.J.A. Steel, O. Hemmings, A. O'Byrne, N. Kouphou, R.P. Galao, G. Betancor, H.D. Wilson, A.W. Signell, H. Winstone, C. Kerridge, I. Huet-

tner, J.M. Jimenez-Guardeño, M.J. Lista, N. Temperton, L.B. Snell, K. Bisnauthsing, A. Moore, A. Green, L. Martinez, B. Stokes, J. Honey, A. Izquierdo-Barras, G. Arbane, A. Patel, M.K.I. Tan, L. O'Connell, G. O'Hara, E. MacMahon, S. Douthwaite, G. Nebbia, R. Batra, R. Martinez-Nunez, M. Shankar-Hari, J.D. Edgeworth, S.J.D. Neil, M.H. Malim, and K.J. Doores. Longitudinal observation and decline of neutralizing antibody responses in the three months following SARS-CoV-2 infection in humans. *Nature Microbiology*, 5:1598–1607, 2020.

[2] H. Ma, W. Zeng, H. He, D. Zhao, D. Jiang, P. Zhou, L. Cheng, Y. Li, Ma X., and T. Jin. Serum iga, igm, and igg responses in covid-19. *Cell. Mol. Immunol.*, 17:773–775, 2020.

[3] J. Klingler, S. Weiss, V. Itri, X. Liu, K.Y. Oguntuyo, C. Stevens, S. Ikegame, C.T. Hung, G. Enyindah-Asonye, F. Amanat, I. Baine, S. Arinsburg, J.C. Bandres, E.M. Kojic, J. Stoever, D. Jurczyszak, M. Bermudez-Gonzalez, A. Nádas, S. Liu, B. Lee, S. Zolla-Pazner, and C.E. Hioe. Role of immunoglobulin m and a antibodies in the neutralization of severe acute respiratory syndrome coronavirus 2. *J Infect Dis.*, 223(6):957–970, 2021.

[4] M. Huang, Q.B. Lu, H. Zhao, Y. Zhang, Z. Sui, L. Fang, D. Liu, X. Sun, K. Peng, W. Liu, and W. Guan. Temporal antibody responses to SARS-CoV-2 in patients of coronavirus disease 2019. *Cell Discovery*, 6(64), 2020.

[5] Q-X. Long, B-Z. Liu, H-J. Deng, G-C. Wu, K. Deng, Y-K. Chen, P. Liao, J-F. Qiu, Y. Lin, X-F. Cai, D-Q. Wang, Y. Hu, J-H. Ren, N. Tang, Y-Y. Xu, L-H. Yu, Z. Mo, F. Gong, X-L. Zhang, W-G. Tian, L. Hu, X-X. Zhang, J-L. Xiang, H-X. Du, H-W. Liu, C-H. Lang, X-H. Luo, S-B. Wu, X-P. Cui, Z. Zhou, M-M. Zhu, J. Wang, C-J. Xue, X-F. Li, L. Wang, Z-J. Li, K. Wang, C-C. Niu, Q-J. Yang, X-J. Tang, Y. Zhang, X-M. Liu, J-J. Li, D-C. Zhang, F. Zhang, P. Liu, J. Yuan, Q. Li, J-L. Hu, J. Chen, and A-L. Huang. Antibody responses to SARS-CoV-2 in patients with COVID-19. *Nature Medecine*, 26:845–848, 2020.

[6] S. Pickering, G. Betancor, R.P. Galao, B. Merrick, A.W. Signell, H.D. Wilson, M.K.I. Tan, J. Seow, C. Graham, S. Acors, N. Kouphou, K.J.A. Steel, O. Hemmings, A. Patel, G. Nebbia, S. Douthwaite, L. O'Connell, J. Luptak, L.E. McCoy, P. Brouwer, M.J. Van Gils, R. Sanders, Martinez-Nunez, K. Bisnauthsing, G. O'Hara, E. MacMahon, R. Batra, M.H. Malim, S.J.D. Neil, K.J. Doores, and J.D. Edgeworth. Comparative assessment of multiple covid-19 serological technologies supports continued evaluation of point-of-care lateral flow assays in hospital and community healthcare settings. *PLOS Pathogens*, pages 1–19, 2020.

[7] J. Zhao, Q. Yuan, H. Wang, W. Liu, X. Liao, Y. Su, X. Wang, J. Yuan, T. Li, J. Li, S. Qian, C. Hong, F. Wang, Y. Liu, Z. Wang, Q. He, Z. Li, B. He, T. Zhang, Y. Fu, S. Ge, L. Liu, J. Zhang, Xia. N., and Z. Zhang. Antibody responses to sars-cov-2 in patients with novel coronavirus disease 2019. *Clin Infect Dis.*, 71(7):2027–2034, 2020.

[8] S.E. Amjadi, M.F. ans O'Connell, T. Armbrust, S.R. Mergaert, A.M. ans Narpala, Halfmann P.J., C.R. ans Heffron A.S. Bashar, S.J. ans Glover, A. Taylor, D.H.a nd Kawaoka Y. Flach, B.a nd O'Connor, A.K. McDermott, A.B. ans Sethi, and Shelef M.A. Specific covid-19 symptoms correlate with high antibody levels against sars-cov-2. *Immunohorizons*, 5(6):466–476, 2021.

[9] B. Bosnjak, S.C. Stein, S. Willenzon, K. Cordes, W. Puppe, G. Bernhardt, I. Ravens, C. Ritter, R. Schultze-Florey, N. Gödecke, J. Martens, H. Kleine-Weber, M. Hoffmann, A. Cossmann, M. Yilmaz, I. Pink, M.M. Hoeper, G.M.N. Behrens, S. Pöhlmann, Blasczyk R., T.F. Schulz, and R. Förster. Low-serum neutralizing anti-sars-cov-2 antibody levels in midly affected covid-19 convalescent patients revealed by two different detection methods. *Cell. Mol. Immunol.*, 18:936–944, 2021.

[10] D.A. Castillo-Olivares, J. ans Wells, M. Ferrari, A.C.Y. Chan, P. Smith, A. Nadesalingam, Paloniemi M., G.W. Carnell, L. Ohlendorf, D. Cantoni, M. Mayora-Neto, P. Palmer, P. Tonks, N.J. ans Peterhoff D. Temperton, Neckermann P., R. Wagner, R. Doffinger, S. Kempster, A.D. Otter, A. Semper, T. Brooks, A. Albecka, James L.C., M. Page, W. Schwaeble, and J.L. Baxendale, H. ans Heeney. Analysis of serological biomarkers of sars-cov-2 infection in convalescent samples from severe, moderate and mild covid-19 cases. *Front Immunol.*, 19(12), 2021.

[11] D. Herrington. Duration of SARS-CoV-2 Sero-Positivity in a Large Longitudinal Sero-Surveillance. Preprint, MedRxiv, Wake Forest University School of Medicine, 2021.

[12] K.L. Lynch, J.D. Whitman, N.P. Lacanienta, E.W. Beckerdite, S.A. Kastner, B.R. Shy, G.M. Goldgof, A.G. Levine, S.P. Bapat, S.L. Stramer, J.H. Esensten, A.W. Hightower, C. Bern, and A.H.B. Wu. Magnitude and kinetics of anti-severe acute respiratory syndrome coronavirus 2 antibody

responses and their relationship to disease severity. *Clin Infect Dis.*, 72(2):301–308, 2021.
[13] J. Hendriks, R. Schasfoort, M. Koerselman, M. Dannenberg, A.D. Cornet, A. Beishuizen, J. van der Palen, J. Krabbe, A.H.L. Mulder, and M. Karperien. High titers of low affinity antibodies in covid-19 patients are associated with disease severity. *Front. Immunol.*, 13, 2022.
[14] D.S. Khoury, A.K. Wheatley, M.D. Ramuta, A. Reynaldi, D. Cromer, K. Subbarao, D.H. O'Connor, S.J. Kent, and M.P. Davenport. Measuring immunity to SARS-CoV-2 infection: comparing assays and animal models. *Nature Reviews Immunology*, 20:727–738, 2020.
[15] P.-C. Bürkner. Advanced Bayesian Multilevel Modeling with the R Package brms. *The R Journal*, 10(1):395–411, 2018.
[16] C.P. Robert and G. Casella. *Monte Carlo statistical methods.* Springer Verlag, 2004.
[17] P.A. Gelman, J.B. Carlin, H.S. Stern, and D.B. Rubin. *Bayesian Data Analysis.* CRC Press, London, 2003. Second Edition.
[18] J. Gabry, D. Simpson, A. Vehtari, M. Betancourt, and A. Gelman. Visualization in bayesian workflow. *J. Roy. Statist. Soc. Ser. A*, 39:389–402, 2019.
[19] S. Watanabe. Asymptotic equivalence of bayes cross validation and widely applicable information criterion in singular learning theory. *J Mach Learn Res*, 11:3571–3594, 2010.
[20] A. Gelman, J. Hwang, and A. Vehtari. Understanding predictive information criteria for bayesian models. *Stat. Comput.*, 24:997–1016, 2014.
[21] R. Li and S. Nadarajah. A review of student's t distribution and its generalizations. *Empirical economics*, 58:1461–1490, 2020.
[22] R.D. De Veaux. Mixtures of linear regressions. *CSDA*, 8(3):227–245, 1989.
[23] Jordan M.J. and Jacobs R.A. Hierarchical mixtures of linear experts and the em algorithm. *Neural Comput.*, 6(2):181–214, 1994.
[24] Y. Chen, X. Yi, and C. Caramanis. A convex formulation for mixed regression with two components: Minimax optimal rates. In Maria Florina Balcan, Vitaly Feldman, and Csaba SzepesvÃ¡ri, editors, *Proceedings of The 27th Conference on Learning Theory*, volume 35 of *Proceedings of Machine Learning Research*, pages 560–604, Barcelona, Spain, 13–15 Jun 2014. PMLR.
[25] P. Deb and A.M. Holmes. Estimates of use and costs of behavioural health care: a comparison of standard and finite mixture models. *Health economics*, 9(6):475–489, 2000.
[26] K. Viele and B. Tong. Modeling with mixtures of linear regressions. *Statist. Comput.*, 12(4):315–330, 2002.
[27] A.X. Carvalho and M.A. Tanner. Mixtures-of-experts of autoregressive time series: asymptotic normality and model specification. *Neural Networks*, 16(1):39–56, 2005.
[28] W.E. Harrington, O. Trakhimets, D.V. Andrade, N. Dambrauskas, A. Raappana, Y. Jiang, J. Houck, W. Selman, A. Yang, V. Vigdorovich, W. Yeung, M. Haglund, J. Wallner, A. Oldroyd, S. Hardy, S.W.-A. Stewart, A. Gervassi, W.V. Voorthis, L. Frenckel, and D.N. Sather. Rapid decline of neutralizing antibodies is associated with decay of igm in adults recovered form mild covid-19. *Cell Reports Medicine*, 2:1–9, 2021.
[29] M.M. Patel, N.J. Thornburg, W.B. Stubblefield, H.K. Talbot, M.M. Coughlin, L.R. Feldstein, and W.H. Self. Change in antibodies to sars-cov-2 over 60 days among health care personnel in nashville, tennessee. *JAMA*, 324(17):1781–1782, 2020.
[30] M. Nairz, S. Sahanic, A. Pizzini, A. Böhm, P. Tymoszuk, A.-M. Mitterstiller, L. Von Raffay, P. Grubwieser, R. Bellmann-Weiler, S. Koppelstätter, A. Schroll, D. Haschka, M. Zimmermann, S. Blunder, K. Trattnig, H. Naschberger, W. Klotz, I. Theurl, V. Petzer, C. Gehrer, J.E. Mindur, A. Luger, C. Schwabl, G. Widmann, G. Weiss, J. Löffler-Ragg, I. Tancevski, and T. Sonnweber. Quantity of igg response to sars-cov-2 spike glycoprotein predicts pulmonary recovery from covid-19. *Sci. Rep.*, 12(3677):3202–3208, 2022.
[31] R. Yang, X. Gui, and Y. Xiong. Comparison of Clinical Characteristics of Patients with Asymptomatice vs Symptomatic Coronavirus Disease 2019 in Wuhan, China. *JAMA Network Open*, 3(5), 2020.
[32] R.K. Starke, D. Reissig, G. Petereit-Haack, S. Schmauder, A. Nienhaus, and A. Seidler. The isolated effect of age on the risk of covid-19 severe outcomes: a systematic review with meta-analysis. *BMJ Global Health*, 6(12):503–522, 2021.
[33] Y. Statsenko, F. Al Zahmi, T. Habuza, T.M. Almansoori, D. Smetanina, G.L. Simiyu, K. Neidl-Van Gorkom, M. Ljubisavljevic, R. Awawdeh, H. Elshekhali, M. Lee, N. Salamin, R. Sajid, D. Kiran,

S. Nihalani, T. Loney, A. Bedson, A. Dehdashtian, and J. Al Koteesh. Impact of age and sex on covid-19 severity assessed from radiologic and clinical findings. *Frontiers in Cellular and Infection Microbiology*, 11, 2022.

Tables

Titer	WAIC (BLM)	(BMLM)	looAIC (BLM)	(BMLM)
IgG	845.9	512	858.8	539
IgM	659.5	377.5	683	413.2
IgA	874.3	632.8	894.1	645.2
Id50	1021.8	938.8	1040.4	958

Table 1. Models comparison criteria for the four titers.

Severity score	IgG	IgM	IgA	ID50
"0 vs 1/2/3"	0.57 [0.43; 0.70]	**0.65** [0.53; 0.76]	**0.67** [0.55; 0.78]	0.57 [0.47; 0.67]
"0 vs 4"	0.62 [0.47; 0.75]	**0.72** [0.62; 0.82]	**0.73** [0.63; 0.82]	**0.84** [0.78; 0.90]
"0 vs 5"	0.67 [0.46; 0.86]	0.65 [0.49; 0.79]	**0.77** [0.64; 0.89]	**0.87** [0.77; 0.95]
"1/2/3 vs 4"	0.53 [0.42; 0.64]	0.57 [0.45; 0.68]	0.56 [0.45; 0.67]	**0.78** [0.70; 0.84]
"1/2/3 vs 5"	0.59 [0.42; 0.75]	0.49 [0.33; 0.64]	0.59 [0.44; 0.74]	**0.76** [0.65; 0.86]
"4 vs 5"	0.57 [0.39; 0.74]	0.41 [0.26; 0.56]	0.54 [0.40; 0.67]	0.39 [0.29; 0.49]

Table 2. Comparison probabilities of maximum amplitude between severity scores. The probability of an SS_k patient having a lower amplitude than an SS_l patient was calculated by averaging over the M draws and over all SS_k vs SS_l patient pairs, the number of times an SS_k patient has a lower maximum value than an SS_l patient, where $k < l$. The main value stands for the mean, specified with a credibility interval at level 80%. When the interval does not contain 0.5, then titers value is significantly lower for patients with severity score SS_k than those with SS_l. More precisely, an SS_k patient is considered to have a significantly lower amplitude than an SS_l patient if the 10%-quantile, over the M draws, of the proportion of times an SS_k patient has a lower amplitude value than an SS_l patient, among all pairs of SS_k vs SS_l patients, exceeds 0.5. Red bold values stand for significant probabilities.

Titer	Severity score	30 days	60 days	90 days	180 days
IgG	**"0"**	0.19 [0.13; 0.24]	0.15 [0.09; 0.22]	0.32 [0.17; 0.46]	0.78 [0.60; 0.94]
	"1/2/3"	0.20 [0.14; 0.25]	0.16 [0.08; 0.25]	0.23 [0.09; 0.40]	0.72 [0.56; 0.88]
	"4"	0.16 [0.10; 0.22]	0.13 [0.06; 0.20]	0.19 [0.07; 0.32]	0.75 [0.58; 0.89]
	"5"	0.15 [0.08; 0.22]	0.13 [0.04; 0.22]	0.19 [0.05; 0.32]	0.64 [0.40; 0.86]
	"GLOBAL"	0.17 [0.13; 0.22]	0.14 [0.08; 0.21]	0.23 [0.11; 0.36]	0.74 [0.58; 0.87]
IgM	**"0"**	0.16 [0.12; 0.21]	0.25 [0.18; 0.33]	0.51 [0.38; 0.63]	0.79 [0.65; 0.93]
	"1/2/3"	0.12 [0.08; 0.17]	0.16 [0.10; 0.24]	0.37 [0.24; 0.49]	0.77 [0.61; 0.92]
	"4"	0.10 [0.07; 0.15]	0.14 [0.09; 0.20]	0.40 [0.28; 0.51]	0.87 [0.76; 0.96]
	"5"	0.11 [0.06; 0.16]	0.16 [0.08; 0.25]	0.39 [0.24; 0.54]	0.79 [0.61; 0.98]
	"GLOBAL"	0.12 [0.09; 0.16]	0.18 [0.13; 0.23]	0.42 [0.31; 0.52]	0.82 [0.71; 0.92]
IgA	**"0"**	0.39 [0.33; 0.45]	0.58 [0.50; 0.66]	0.70 [0.57; 0.83]	0.81 [0.61; 0.97]
	"1/2/3"	0.27 [0.21; 0.33]	0.32 [0.23; 0.41]	0.52 [0.36; 0.69]	0.78 [0.59; 0.95]
	"4"	0.23 [0.17; 0.28]	0.26 [0.20; 0.33]	0.52 [0.39; 0.66]	0.80 [0.62; 0.94]
	"5"	0.21 [0.15; 0.27]	0.22 [0.12; 0.32]	0.49 [0.30; 0.67]	0.80 [0.59; 0.99]
	"GLOBAL"	0.27 [0.22; 0.32]	0.34 [0.28; 0.41]	0.56 [0.43; 0.69]	0.80 [0.62; 0.93]
ID50	**"0"**	0.15 [0.10; 0.20]	0.21 [0.14; 0.29]	0.47 [0.35; 0.59]	0.52 [0.40; 0.68]
	"1/2/3"	0.18 [0.13; 0.23]	0.23 [0.14; 0.33]	0.46 [0.33; 0.59]	0.53 [0.41; 0.69]
	"4"	0.05 [0.03; 0.08]	0.11 [0.06; 0.16]	0.38 [0.28; 0.48]	0.54 [0.42; 0.69]
	"5"	0.01 [0.00; 0.04]	0.09 [0.02; 0.18]	0.39 [0.26; 0.50]	0.53 [0.40; 0.70]
	"GLOBAL"	0.10 [0.08; 0.13]	0.17 [0.11; 0.23]	0.43 [0.32; 0.53]	0.53 [0.42; 0.67]

Table 3. POD by severity score at specific moments, accounting for its long-term evolution. Results are given by titer at 30, 60, 90 and 180 days. The main value stands for $POD_{SS_k}(t)$, specified with a sample interval at level 80%. In other words, at each time t, the mean and quantiles at 10% and 90% are calculated from the M draws $POD^{(m)}_{SS_k}(t)$. Moreover, lines "GLOBAL" give $POD(t)$ values, specified with their associated 80%-credibility interval, computed as quantile samples of $POD^{(m)}$.

Figures and figure captions

Figure captions

Figure 1. Evolution of log-transformed titer values over time post onset symptoms. Every curve represents one individual. The horizontal darkred line, represents the associated threshold for sero-positivity. Top-Left: IgG_S ; Top-Right: IgM_S ; Bottom-Left: IgA_S ; Bottom-Right: Id50_PV titer.

Figure 2. Posterior predictive checks for IgG, IgM, IgA and ID50 titers. 10 simulations are drawn from the posterior predictive distribution, induced either by the (BLM), left-hand side, or by the (MBLM), right-hand side. Using a Gaussian kernel, replicated simulations density (y_{rep} in light red) are compared with the observed density (y in black).

Figure 3. Membership probabilities by severity scrore assignment. Top-Left: IgG_S titer Top-Right: IgM_S titer Bottom-Left: IgA_S titer Bottom-Right: Id50_PV titer.

Figure 4. Predicted evolution of titers, averaged by severity score assignment. Top-Left: IgG_S titer Top-Right: IgM_S titer Bottom-Left: IgA_S titer Bottom-Right: Id50_PV titer.

Figure 5. ROC curves for IgG (dotted line), IgM (solid line) and IgA (dashed line) titers. Circles show the optimal seropositivity limit for every titer, in contrast with squares that show the usual one.

Figure 6. Evolution of the probability of being out of detection for sero-positivity, averaged by severity scrore assignment. Top-Left: IgG_S titer Top-Right: IgM_S titer Bottom-Left: IgA_S titer Bottom-Right: Id50_PV titer.

Figure 7. Evolution of comparison probabilities between severity scores. The probability of an SS_k patient having a higher POD than an SS_l patient was calculated by averaging over the M draws and over all the SS_k vs SS_l patient pairs, the proportion of times an SS_k patient has a higher POD than an SS_l patient, where $k < l$. Top-Left: IgG_S titer Top-Right: IgM_S titer Bottom-Left: IgA_S titer Bottom-Right: Id50_PV titer.

Figures

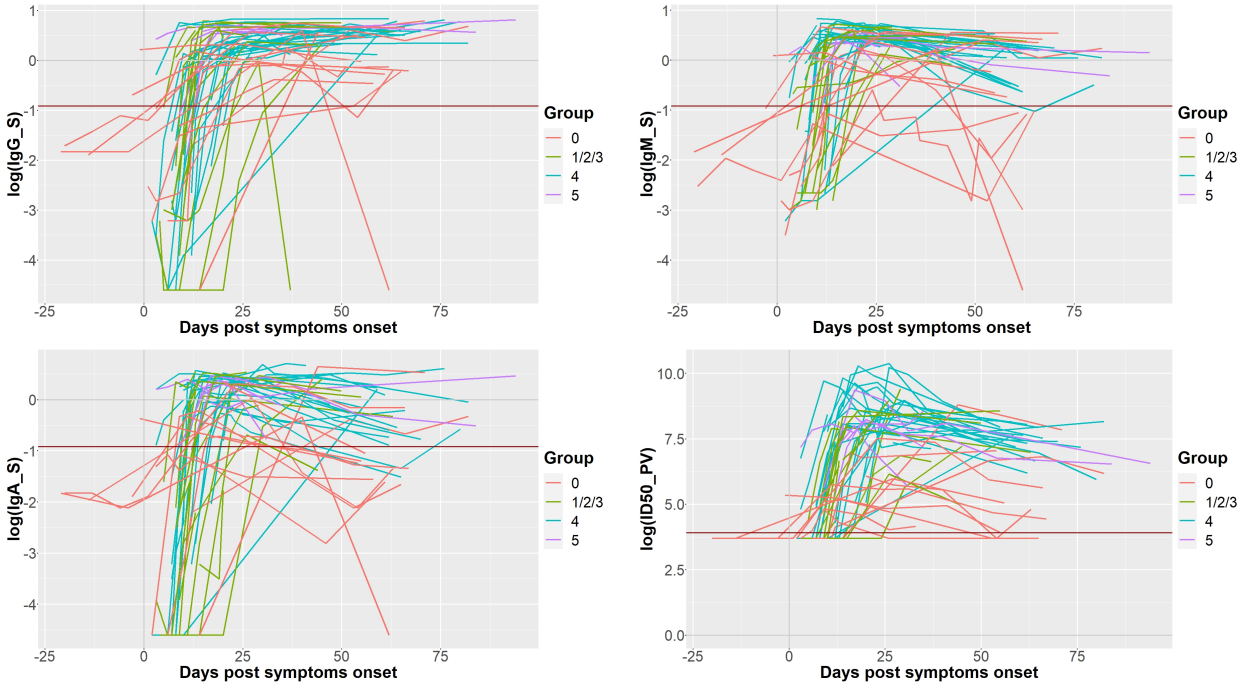

Figure 1. Evolution of log-transformed titer values over time post onset symptoms. Every curve represents one individual. The horizontal darkred line, represents the associated threshold for sero-positivity. Top-Left: IgG_S ; Top-Right: IgM_S ; Bottom-Left: IgA_S ; Bottom-Right: Id50_PV titer.

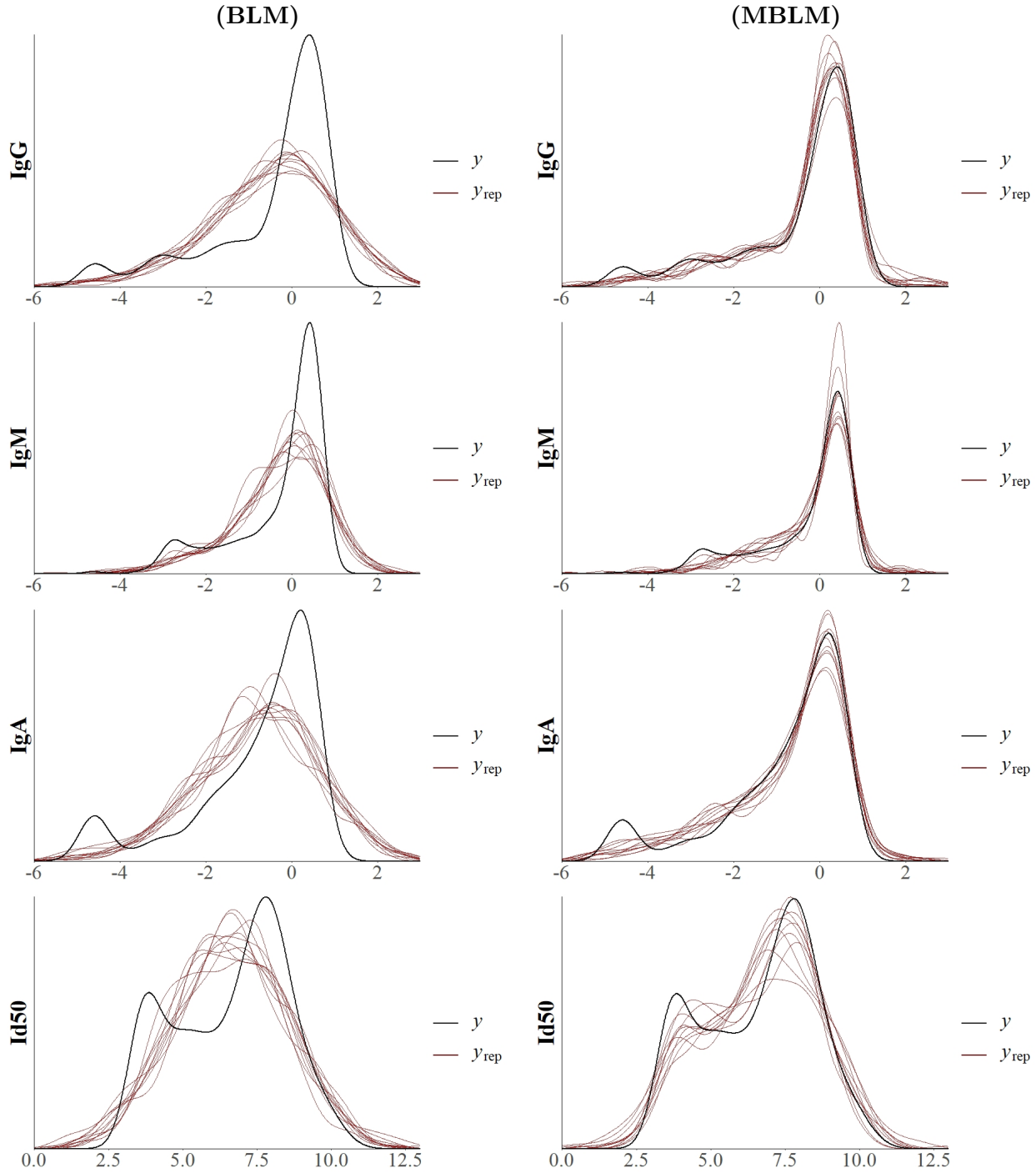

Figure 2. Evolution of log-transformed titer values over time post onset symptoms. Every curve represents one individual. The horizontal darkred line, represents the associated threshold for sero-positivity. Top-Left: IgG_S ; Top-Right: IgM_S ; Bottom-Left: IgA_S ; Bottom-Right: Id50_PV titer.

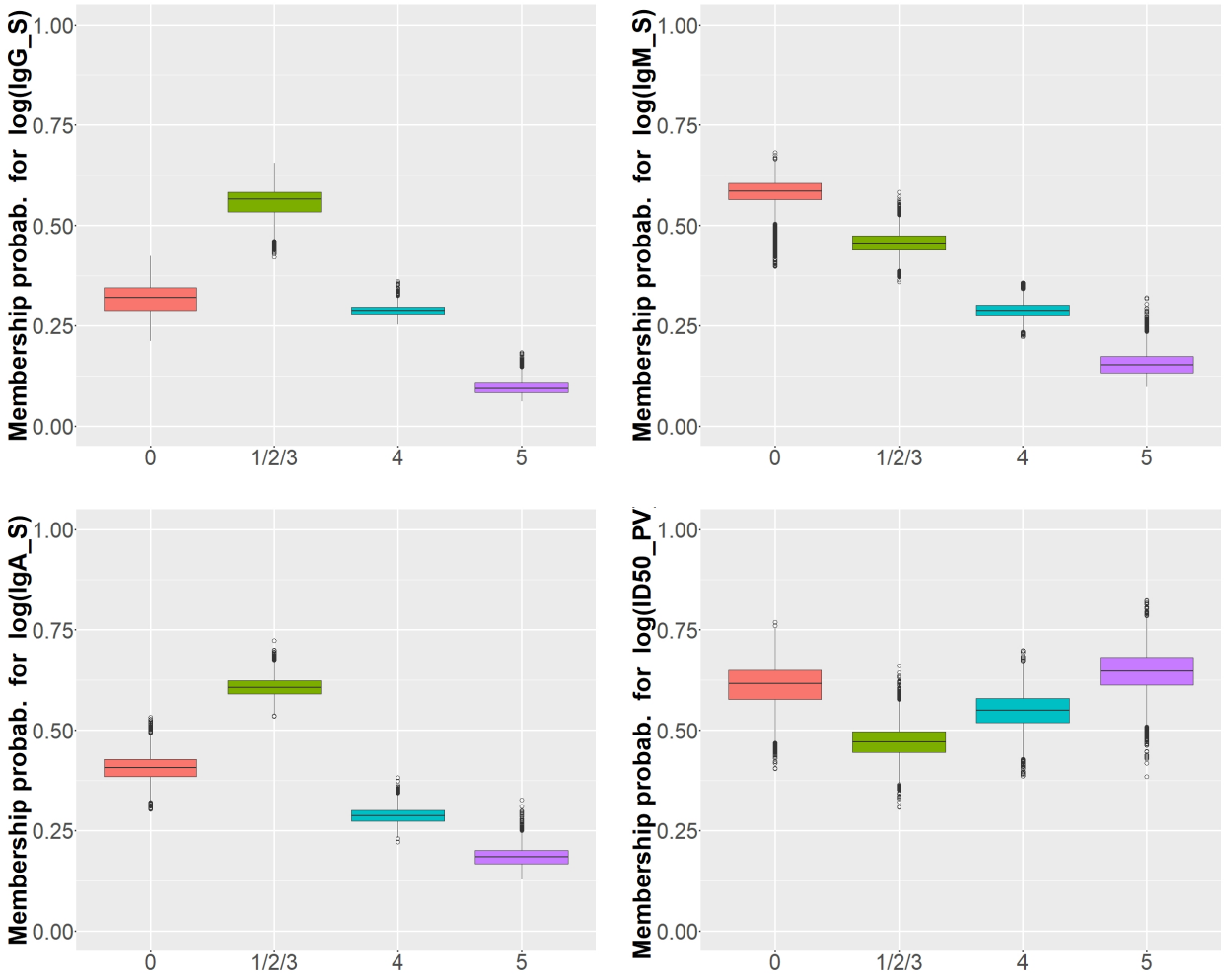

Figure 3. Membership probabilities by severity scrore assignment. Top-Left: IgG_S titer Top-Right: IgM_S titer Bottom-Left: IgA_S titer Bottom-Right: Id50_PV titer.

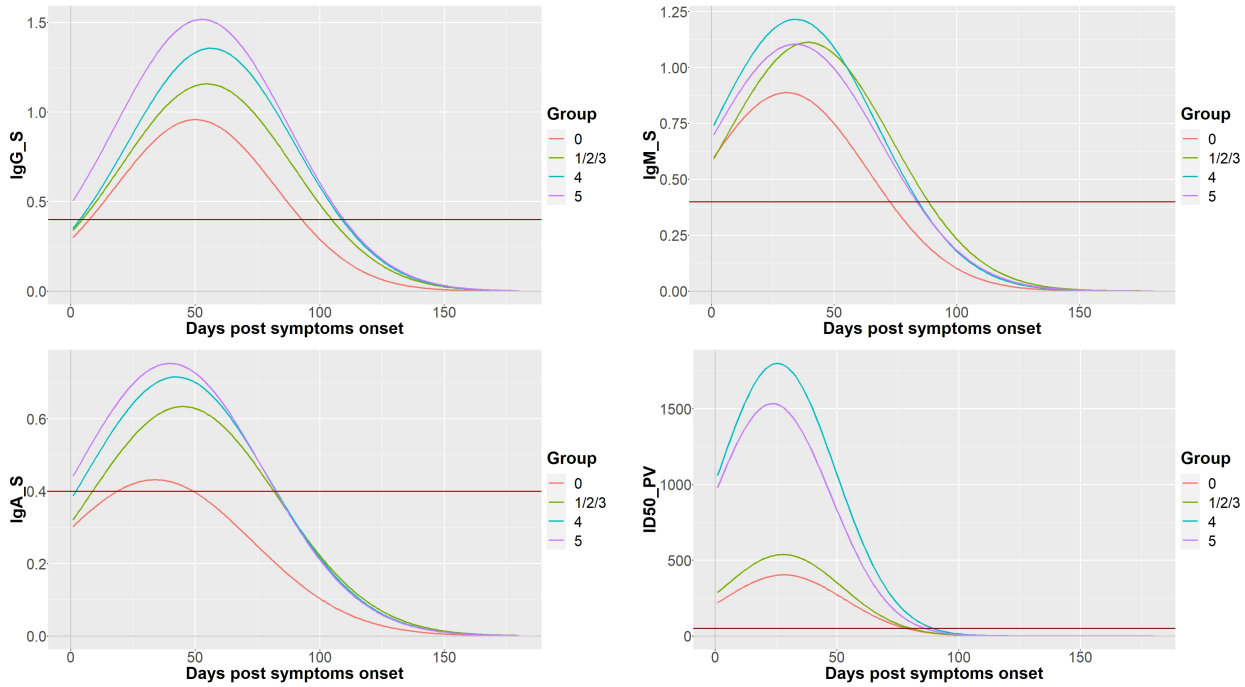

Figure 4. Posterior predictive checks for IgG, IgM, IgA and ID50 titers. 10 simulations are drawn from the posterior predictive distribution, induced either by the (BLM), left-hand side, or by the (MBLM), right-hand side. Using a Gaussian kernel, replicated simulations density (y_{rep} in light red) are compared with the observed density (y in black).

Figure 5.

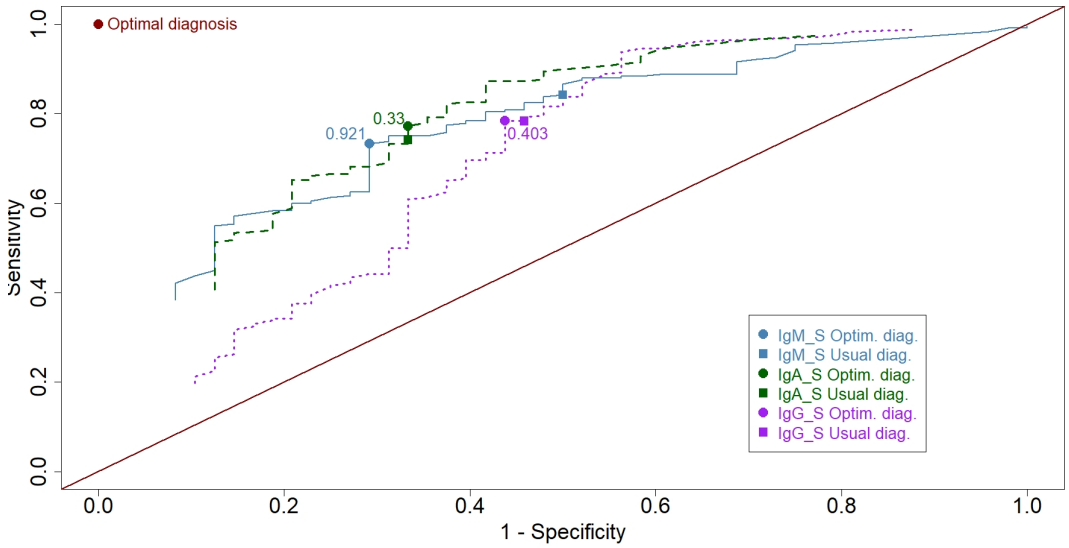

Figure 5. ROC curves for IgG (dotted line), IgM (solid line) and IgA (dashed line) titers. Circles show the optimal seropositivity limit for every titer, in contrast with squares that show the usual one.

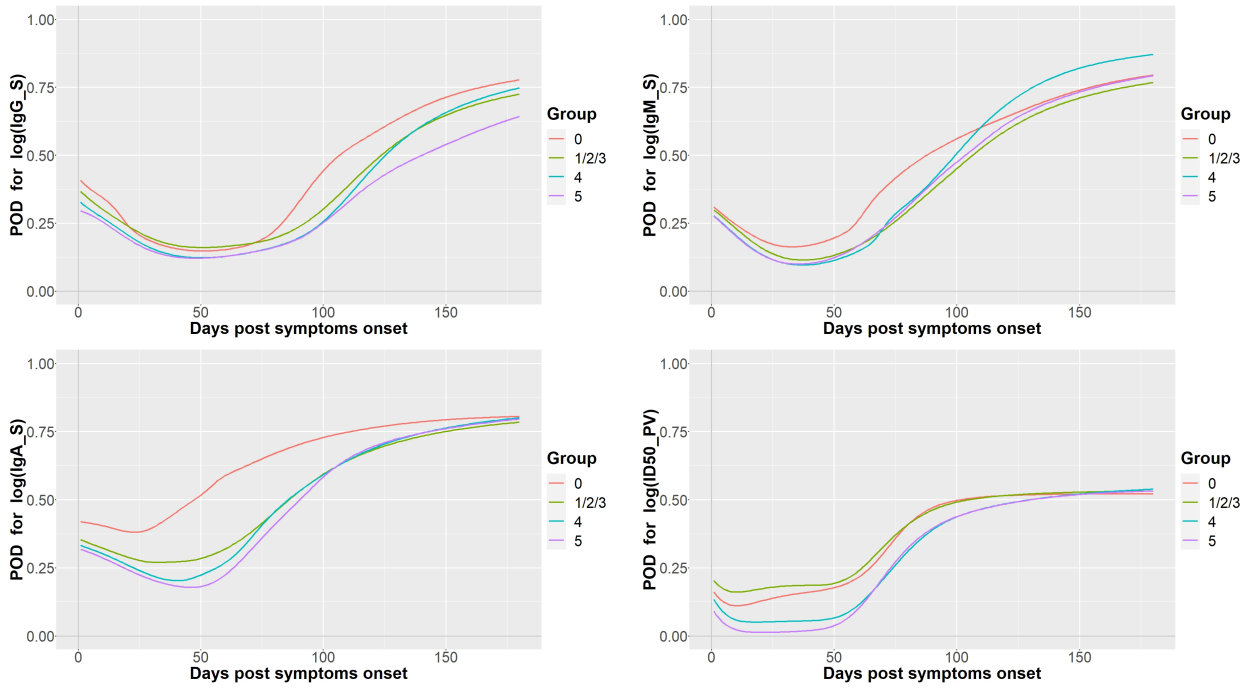

Figure 6. Evolution of the probability of being out of detection for sero-positivity, averaged by severity scrore assignment. Top-Left: IgG_S titer Top-Right: IgM_S titer Bottom-Left: IgA_S titer Bottom-Right: Id50_PV titer.

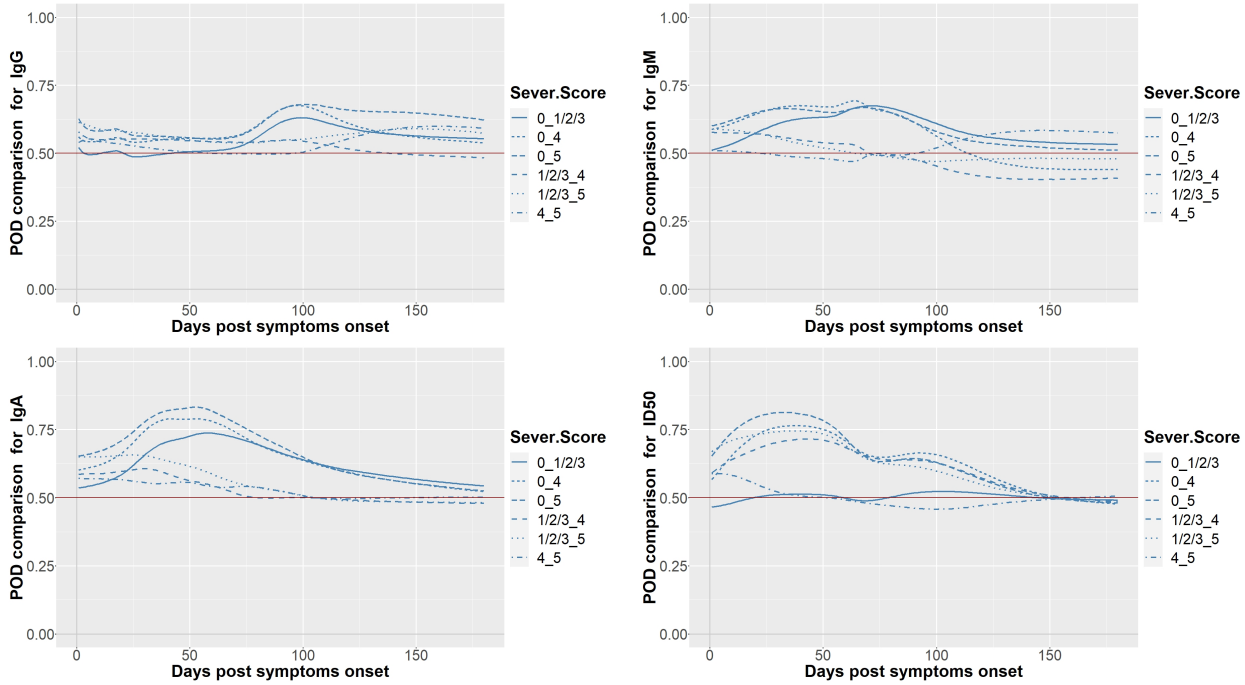

Figure 7. Evolution of comparison probabilities between severity scores. The probability of an SS_k patient having a higher POD than an SS_l patient was calculated by averaging over the M draws and over all the SS_k vs SS_l patient pairs, the proportion of times an SS_k patient has a higher POD than an SS_l patient, where $k < l$. Top-Left: IgG_S titer Top-Right: IgM_S titer Bottom-Left: IgA_S titer Bottom-Right: Id50_PV titer.

Supplementary material of
Bayesian approach to infer the duration of antibody seropositivity and neutralizing responses to SARS-CoV-2

Manuela Royer-Carenzi[1] and Jean-Marc Freyermuth[1]

[1] Aix Marseille Univ, CNRS, Centrale Marseille, I2M, Marseille, France

ARTICLE HISTORY
Compiled January 29, 2023

Contents

S1 Additional analysis for POD **1**
S1.1 POD comparison between severity scores at specific moments 1
S1.2 Evolution of POD comparison between severity scores 1

S1. Additional analysis for POD

S1.1. POD comparison between severity scores at specific moments

In the main manuscript, to determine whether POD difference between severity-score groups is significant, in an accurate way, we use posterior chains to estimate the probabilities that the POD of an SS_k-patient to be higher than the POD of an SS_l-patient, when $k < l$. In other words, at each time t, for any replicate, the probability of an SS_k patient having a higher POD than an SS_l patient was calculated as the proportion of times an SS_k patient has a higher POD than an SS_l patient, over all SS_k vs SS_l patient pairs, where $k < l$. Precisely, we compute the mean such as the 10%- and the 90%-sample quantiles, over the $M = 7\,000$ replicates, of $\Pi_{k \text{ vs } l}^{\text{POD }(m)}(t)$. Table S1 displays POD comparison probabilities between severity scores at specific moments, accounting for their long-term evolution. By displaying values higher than 0.5, Table S1 confirms that the lower the severity score, the higher the POD, in almost all cases. The result is considered as significant as soon as the associated 10%-quantile is also larger than 0.5.

S1.2. Evolution of POD comparison between severity scores

Furthermore, still in manuscript, Figure 7 displays the evolution of the averaged POD comparisons. In Figure S1 we display the evolution of the 10%-quantile associated to the comparison probabilities between severity scores. A severity-score pairs comparison is significant as soon as the associated curve is above the horizontal line $y = 0.5$. We see that for antibody titers, POD is significantly higher for asymptomatic patients with respect to the others up to at least 100 days for IgA, whereas for IgG (resp. IgM), asymptomatic only differ from most severely affected patients (with severerity score "4" or "5"), up to at least 75 days for IgM (resp. around 100 days for IgG). Finally, for ID50, most pairs of severity scores are significantly different since for at least 90% of replications, we have $\Pi_{k \text{ vs } l}^{\text{POD }(m)}(t) > 0.5$, until 60 days for SS_k ="1/2/3" (slighlty

affected patients) versus SS_l ="4" or "5", and even until 100 days for asymptomatic patients versus severely affected patients (SS_l ="4" or "5"). As a conclusion a previous infection by Covid-19 disease leaves traces in terms of antibodies, significantly more easily detectable if the individual has been more severely affected, and this effect lasts around 100 days. With regard to immunity, a previous infection by Covid-19 disease also generates a more pronounced immune response for more severely affected patients, during about 100 days.

Table

Titer	Severity score	30 days	60 days	90 days	180 days
IgG	**"0 vs 1/2/3"**	0.49 [0.37; 0.61]	0.51 [0.38; 0.65]	0.61 [0.47; 0.75]	0.55 [0.44; 0.67]
	"0 vs 4"	0.54 [0.42; 0.66]	0.55 [0.43; 0.68]	**0.66** [0.53; 0.78]	0.54 [0.43; 0.65]
	"0 vs 5"	0.56 [0.40; 0.74]	0.55 [0.37; 0.74]	0.66 [0.48; 0.82]	0.62 [0.43; 0.80]
	"1/2/3 vs 4"	0.55 [0.44; 0.66]	0.54 [0.43; 0.66]	0.55 [0.43; 0.67]	0.48 [0.39; 0.58]
	"1/2/3 vs 5"	0.57 [0.40; 0.73]	0.54 [0.36; 0.71]	0.55 [0.36; 0.72]	0.57 [0.40; 0.73]
	"4 vs 5"	0.52 [0.35; 0.69]	0.5 [0.33; 0.67]	0.5 [0.33; 0.67]	0.59 [0.41; 0.75]
IgM	**"0 vs 1/2/3"**	0.61 [0.49; 0.73]	**0.65** [0.53; 0.78]	**0.64** [0.53; 0.75]	0.53 [0.40; 0.66]
	"0 vs 4"	**0.67** [0.56; 0.77]	**0.68** [0.58; 0.78]	**0.62** [0.52; 0.72]	0.44 [0.32; 0.56]
	"0 vs 5"	**0.66** [0.51; 0.81]	0.66 [0.49; 0.81]	0.62 [0.47; 0.76]	0.51 [0.37; 0.66]
	"1/2/3 vs 4"	0.56 [0.45; 0.67]	0.53 [0.41; 0.66]	0.48 [0.36; 0.60]	0.41 [0.29; 0.52]
	"1/2/3 vs 5"	0.56 [0.39; 0.71]	0.51 [0.33; 0.69]	0.48 [0.32; 0.64]	0.48 [0.34; 0.63]
	"4 vs 5"	0.49 [0.34; 0.65]	0.47 [0.31; 0.63]	0.50 [0.35; 0.65]	0.58 [0.43; 0.71]
IgA	**"0 vs 1/2/3"**	**0.65** [0.54; 0.76]	**0.74** [0.65; 0.82]	**0.67** [0.54; 0.78]	0.54 [0.40; 0.69]
	"0 vs 4"	**0.74** [0.63; 0.83]	**0.78** [0.71; 0.86]	**0.67** [0.56; 0.76]	0.52 [0.38; 0.66]
	"0 vs 5"	**0.77** [0.65; 0.89]	**0.82** [0.71; 0.91]	**0.69** [0.54; 0.84]	0.53 [0.35; 0.70]
	"1/2/3 vs 4"	**0.61** [0.50; 0.71]	0.55 [0.44; 0.65]	0.50 [0.39; 0.61]	0.48 [0.37; 0.59]
	"1/2/3 vs 5"	**0.66** [0.50; 0.81]	0.59 [0.43; 0.75]	0.53 [0.36; 0.69]	0.48 [0.32; 0.65]
	"4 vs 5"	0.56 [0.40; 0.71]	0.54 [0.39; 0.69]	0.53 [0.39; 0.66]	0.50 [0.36; 0.65]
ID50	**"0 vs 1/2/3"**	0.51 [0.42; 0.60]	0.50 [0.38; 0.62]	0.52 [0.38; 0.65]	0.49 [0.39; 0.59]
	"0 vs 4"	**0.76** [0.67; 0.84]	**0.71** [0.61; 0.81]	**0.66** [0.52; 0.80]	0.48 [0.34; 0.61]
	"0 vs 5"	**0.81** [0.70; 0.92]	**0.73** [0.56; 0.88]	0.64 [0.45; 0.82]	0.48 [0.33; 0.63]
	"1/2/3 vs 4"	**0.7** [0.62; 0.78]	**0.69** [0.6; 0.78]	**0.64** [0.51; 0.76]	0.49 [0.37; 0.60]
	"1/2/3 vs 5"	**0.74** [0.63; 0.85]	**0.70** [0.55; 0.83]	0.62 [0.45; 0.78]	0.49 [0.35; 0.63]
	"4 vs 5"	0.52 [0.39; 0.66]	0.49 [0.35; 0.64]	0.46 [0.31; 0.62]	0.51 [0.39; 0.62]

Table S1. Comparison probabilities between severity scores at specific moments. The probability of an SS_k patient having a higher POD than an SS_l patient was calculated by averaging over the 7 000 replicates and over all SS_k vs SS_l patient pairs, the proportion of times an SS_k patient has a higher POD than an SS_l patient, where $k < l$. Results are given by titer, displaying all lines "SS_k vs SS_l", at times 30, 60, 90 and 180 days. The main value stands for the $\Pi^{\text{POD}}_{k \text{ vs } l}(t)$, specified with a credibility interval at level 80%. When the interval does not contain 0.5, then POD value is significantly higher for patients with severity score SS_k than those with SS_l. More precisely, an SS_k patient is considered to have a significantly higher POD than an SS_l patient if the 10%-quantile over 7 000 replicates of the proportion of times an SS_k patient has a lower POD value than an SS_l patient, among all pairs of SS_k vs SS_l patients, exceeds 0.5. Red bold values stand for significant probabilities.

Figure

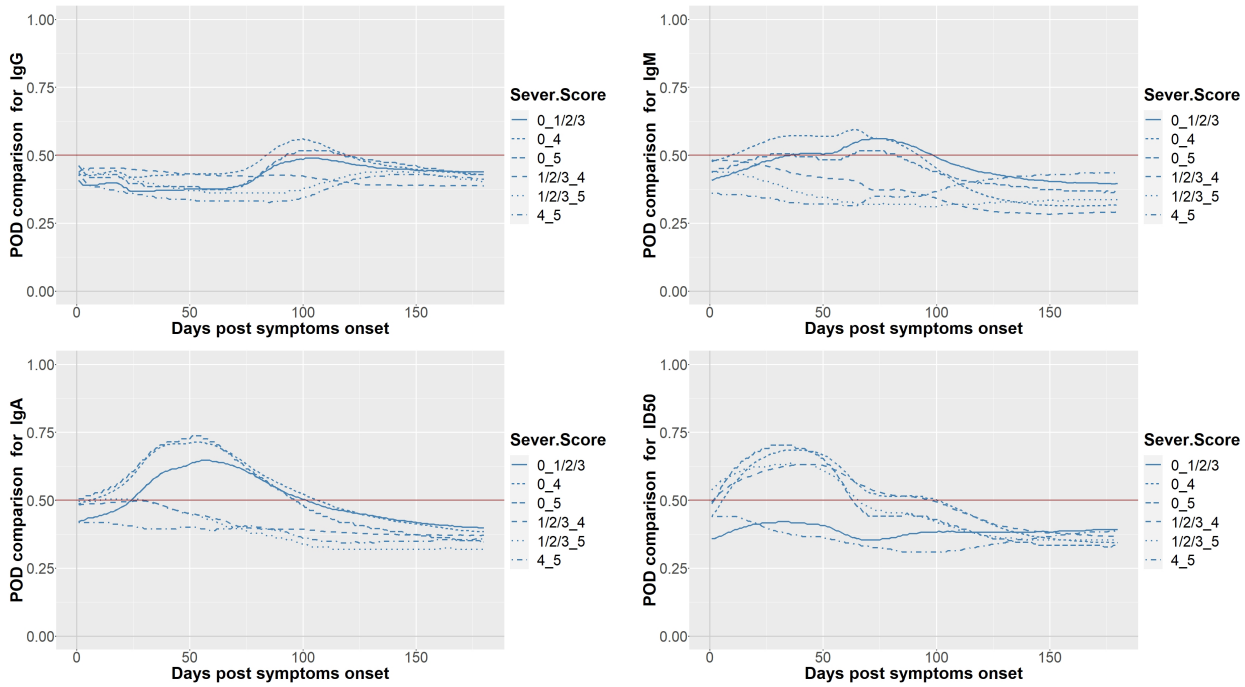

Figure S1. Evolution of the 10%-quantile associated to the comparison probabilities between severity scores. An SS_k patient is considered to have a significantly higher POD than an SS_l patient if the 10%-quantile over 7 000 replicates of the proportion of times an SS_k patient has a lower POD value than an SS_l patient, among all pairs of SS_k vs SS_l patients, exceeds 0.5. Top-Left: IgG_S titer Top-Right: IgM_S titer Bottom-Left: IgA_S titer Bottom-Right: Id50_PV titer.